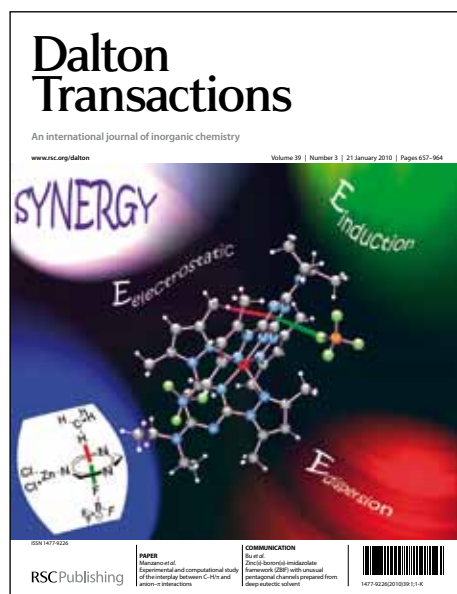


Dalton Transactions

Accepted Manuscript



This is an *Accepted Manuscript*, which has been through the RSC Publishing peer review process and has been accepted for publication.

Accepted Manuscripts are published online shortly after acceptance, which is prior to technical editing, formatting and proof reading. This free service from RSC Publishing allows authors to make their results available to the community, in citable form, before publication of the edited article. This *Accepted Manuscript* will be replaced by the edited and formatted *Advance Article* as soon as this is available.

To cite this manuscript please use its permanent Digital Object Identifier (DOI®), which is identical for all formats of publication.

More information about *Accepted Manuscripts* can be found in the [Information for Authors](#).

Please note that technical editing may introduce minor changes to the text and/or graphics contained in the manuscript submitted by the author(s) which may alter content, and that the standard [Terms & Conditions](#) and the [ethical guidelines](#) that apply to the journal are still applicable. In no event shall the RSC be held responsible for any errors or omissions in these *Accepted Manuscript* manuscripts or any consequences arising from the use of any information contained in them.

Dinuclear cobalt(II) and cobalt(III) complexes of bis-bidentate naphthoquinone ligands†

Yanyan Mulyana,^a Kerwyn G. Alley,^a Kristian M. Davies,^a Brendan F. Abrahams,^a Boujemaa Moubaraki,^b Keith S. Murray^b and Colette Boskovic^{*a}

The combination of bridging bis-bidentate redox-active ligands derived from 3,3-bis-2-hydroxy-1,4-naphthoquinone (bhnqH₂), ancillary ligands based on tris(2-pyridylmethyl)amine (tpa) and cobalt salts have afforded a new family of dinuclear cobalt complexes. Compounds of the complexes

$[\text{Co}_2(\text{bhnq})(\text{tpa})_2]^{2+}$ (1), $[\text{Co}_2(\text{bhnq})(\text{Metpa})_2]^{2+}$ (2), $[\text{Co}_2(\text{bhnq})(\text{Me}_2\text{tpa})_2]^{2+}$ (3)

$[\text{Co}_2(\text{bhnq})(\text{Me}_3\text{tpa})_2]^{2+}$ (4), $[\text{Co}_2(\text{bhnq})(\text{tpa})_2]^{4+}$ (5), $[\text{Co}_2(\text{bhMenaph})(\text{tpa})_2]^{2+}$ (6) and

$[\text{Co}_2(\text{bhPronaph})(\text{tpa})_2]^{2+}$ (7) (Me_ntpa involves $n = 0, 1, 2$ and 3 methyl groups at the 6-position of the tpa pyridine rings; bhMenaphH₄ = bis-3,4-dihydroxy-4-methoxynaphthalene-1-one; bhPronaphH₄ = bis-3,4-dihydroxy-4-(2-oxopropyl)naphthalen-1(4H)-one) have been characterised by single crystal X-ray

diffraction. While complexes 1-4 possess divalent cobalt centres, trivalent cobalt is evident in complexes 5-7. The bis-bidentate redox-active bridging ligand remains in the diamagnetic quinone bhnq²⁻ redox state in complexes 1-5. Metal-catalysed reaction with methoxide or acetone enolate ions gives rise to the derivatised bridging ligands present in 6 and 7. The electronic properties of compounds of 1-7 have been explored in the solid state by infrared spectroscopy and variable

temperature magnetic measurements and in solution by electronic absorption spectroscopy and cyclic voltammetry.

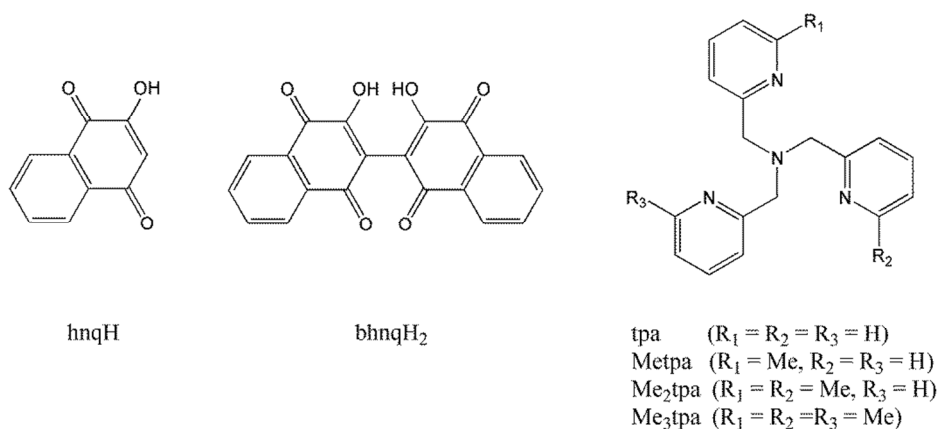
Introduction

Interest in dinuclear cobalt complexes arises in part from their relationship to the active sites of certain metalloenzymes.^{1,2} However, the unique electronic properties of cobalt also confer on cobalt complexes considerable versatility in terms of the ability to act as single-molecule magnets (SMMs) and to display both spin crossover and valence tautomeric transitions.³⁻⁶ Interactions that manifest upon combining pairs of cobalt centres in dinuclear complexes can give rise to novel behaviour, as reported recently for exchange-coupled dinuclear cobalt complexes that can be switched in a single-molecule junction or with dual "ON/OFF" switchability of the SMM behaviour of the oxidised and reduced forms.⁷ Of particular interest to us is the incorporation of redox-active ligands in these complexes, which can allow stimulated intramolecular electron transfer coupled with a spin transition at the cobalt centre in a valence tautomeric transition.⁸⁻¹⁰ Cobalt complexes with redox-active, or "non-innocent" ligands are also of considerable interest for their roles as catalysts of various chemical transformations.¹¹ We have recently reported a family of dinuclear cobalt complexes of formula $[\text{Co}_2(\text{spiro})(\text{Me}_n\text{tpa})_2]^{2+}$ (spiroH₄ = 3,3,3',3'-tetramethyl-1,1'-spirobis(indane-5,5',6,6'-tetrol; Me_ntpa = tris(2-pyridylmethyl)amine (tpa) successively derivatised at the 6-position of the pyridine rings, $n = 0-4$) in which spiroconjugation of the redox-active bis-dioxolene bridging ligand mediates thermally-activated vibronic coupling between the two cobalt-dioxolene moieties, giving rise to a two-step valence tautomeric transition in the Me₂tpa analogue.^{12,13} In order to further explore the origin of the two-step behaviour we are extending our investigation to dinuclear cobalt complexes with other potentially redox-active bridging ligands with varying degrees of electronic conjugation.

An attractive candidate as a potentially redox-active bridging ligand is the doubly deprotonated form of the proligand 3,3-bis-2-hydroxy-1,4-naphthoquinone (bhnqH₂; Chart 1).¹⁴ This molecule can be considered as the dimeric form of the natural product 2-hydroxy-1,4-naphthoquinone (hnqH; Chart 1), commonly known as lawsone, which is the main colouring agent in henna and other dyes. The

deprotonated form of hnqH has been reported to exist in four different redox states: the trianionic catecholate hnq^{3-} , the dianionic monoradical semiquinonate $\text{hnq}^{\bullet 2-}$, the monoanionic quinone hnq^- and the neutral monoradical quinone hnq^\bullet (Scheme S1), although the most commonly observed species is hnq^- .¹⁵⁻²⁸ Coordination complexes of hnq^- have also been reported, of most relevance to this work is a family of mononuclear cobalt(II) complexes of formula $[\text{Co}(\text{hnq})_2(\text{NL})_2]$ and $[\text{Co}(\text{hnq})_2(\text{N}_2\text{L})]$, where NL is pyridine (py) or imidazole and N_2L is 2,2'-bipyridine (2,2'-bpy) or *o*-phenanthroline.²⁹

Chart 1



A number of coordination complexes have been reported in which bhnq^{2-} bridges manganese, cobalt, nickel, copper, zinc or cadmium centres.³⁰⁻³³ These include discrete di-, tri- and tetranuclear complexes and coordination polymers with zig-zag or helical structures. All of these complexes incorporate divalent metal centres, with structural and other evidence suggesting only the dianionic quinone bhnq^{2-} redox state for the ligand. The bhnq^{2-} ligand displays some coordinative flexibility in these complexes, with chelation through the 1,2-positions sometimes accompanied by direct bridging of neighbouring metal centres by the phenoxyl unit.^{32,33} Free rotation around the central carbon-carbon bond also affords considerable variability in the dihedral angle between the two halves of the bhnq^{2-} ligand.

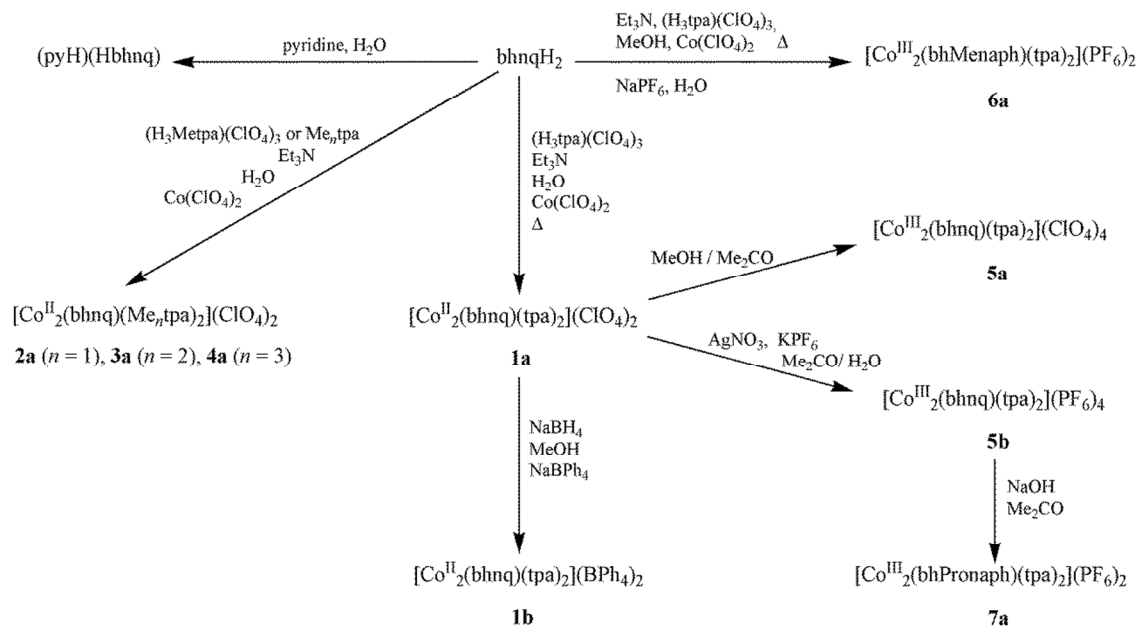
Herein we report the results of our investigation in which we combined ancillary capping ligands derived from tpa with cobalt and bhnqH₂.³⁴ The tpa family of ancillary ligands were selected because successive methylation of the 6-position of the pyridine rings to afford Me_ntpa (*n* = 0, 1, 2 and 3; Chart 1) influences the redox potentials of coordinated metal centres, allowing tuning of the electronic properties of the coordination complexes.^{12,13,35}

Results and discussion

Synthesis

The synthesis of the proligand bhnqH₂ was achieved by radical coupling and dimerisation of hmqH according to a literature procedure.¹⁴ This proligand was subsequently employed for the synthesis of dinuclear cobalt complexes according to the synthetic pathways summarised in Scheme 1. The reaction of stoichiometric amounts of cobalt(II) perchlorate, (H₃tpa)(ClO₄)₃, bhnqH₂ and triethylamine affords a red solid formulated as [Co₂(bhnq)(tpa)₂](ClO₄)₂ (**1a**). Efforts to obtain either an analytically pure bulk sample of **1a**, or single crystals for X-ray diffraction, were unsuccessful. Support for the identity of this compound comes from the ESI mass spectrum in acetonitrile, which displays three main peaks at *m/z* = 694.5, 522.4 and 291.3, corresponding to the fragments {[Co(bhnq)(Htpa)]₂H}²⁺, {Co₂(bhnq)(Htpa)₂}²⁺ and {Htpa}⁺, respectively. Single crystals of the complex [Co₂(bhnq)(tpa)₂]²⁺ (**1**) suitable for X-ray analysis were grown after replacing the perchlorate counteranions with tetraphenylborate, giving [Co₂(bhnq)(tpa)₂](BPh₄)₂·2CH₂Cl₂·2MeOH (**1b**·2CH₂Cl₂·2MeOH), with the partially desolvated bulk sample of **1b**·CH₂Cl₂·2MeOH obtained in 20 % yield. Although it was possible to obtain an analytically pure bulk sample of this compound, reproducibility was challenging, with the purity tending to vary from batch to batch.

Scheme 1

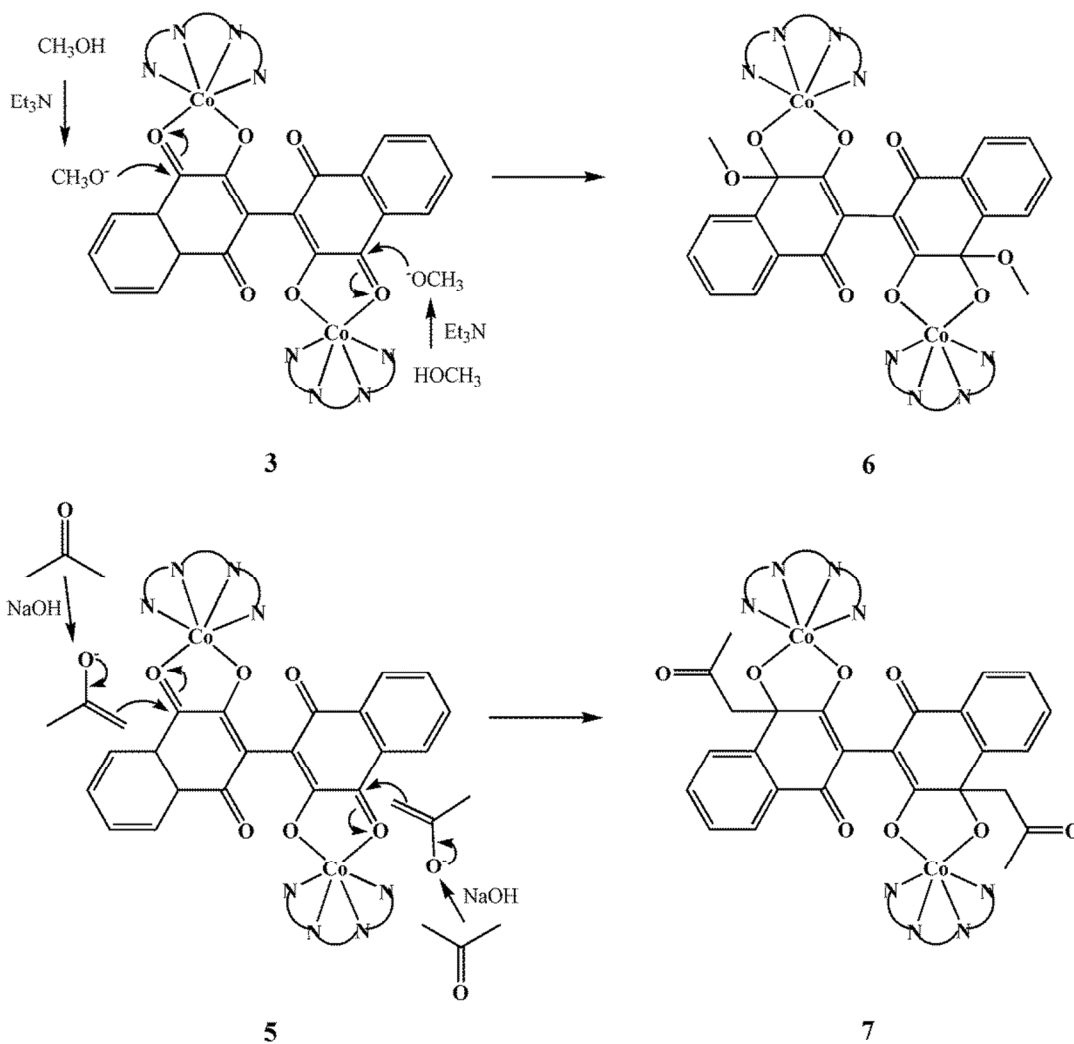


The syntheses of the analogous complexes $[\text{Co}_2(\text{bhnq})(\text{Me}_n\text{tpa})_2]^{2+}$ ($n = 1-3$, **2-4**) with derivatised tpa ligands proceeds more straightforwardly, with analytically pure perchlorate salts readily obtained in 30-60 % yield. A solution of triethylamine and $(\text{H}_3\text{Metpa})(\text{ClO}_4)_3$ was added to a solution of cobalt(II) perchlorate. Addition of the deprotonated bhnq^{2-} ligand affords a red-brown precipitate, which was recrystallised by layering an acetonitrile solution of the crude product with diethyl ether to give purple crystals of $[\text{Co}_2(\text{bhnq})(\text{Metpa})_2](\text{ClO}_4)_2 \cdot 2\text{MeCN} \cdot 2\text{Et}_2\text{O}$ (**2a**·2MeCN·2Et₂O). After air drying, the desolvated sample appeared to be slightly hygroscopic analysing as **2a**·1.5H₂O. In methanol, Me₂tpa or Me₃tpa was added to cobalt(II) perchlorate, followed by bhnq^{2-} , to give a dark red precipitate after approximately 30 minutes. The solid was recrystallised by layering an acetonitrile solution with diethyl ether, yielding purple crystals of $[\text{Co}_2(\text{bhnq})(\text{Me}_2\text{tpa})_2](\text{ClO}_4)_2 \cdot 2\text{MeCN} \cdot \text{H}_2\text{O}$ (**3**·2MeCN·H₂O) and $[\text{Co}_2(\text{bhnq})(\text{Me}_3\text{tpa})_2](\text{ClO}_4)_2 \cdot 2\text{MeCN} \cdot 0.5\text{Et}_2\text{O}$ (**4a**·2MeCN·0.5Et₂O). Air dried samples of these compounds analysed as **3a**·2H₂O and **4a**, respectively.

Aerial oxidation during slow evaporation of a solution of **1a** in acetone/methanol affords red single crystals of the Co(III)-containing compound $[\text{Co}_2(\text{bhnq})(\text{tpa})_2](\text{ClO}_4)_4 \cdot 2\text{MeOH} \cdot 4\text{H}_2\text{O}$ (**5a**·2MeOH·4H₂O), with the air-dried sample obtained in 20% yield and analysing as **5a**·4H₂O. Complex $[\text{Co}_2(\text{bhnq})(\text{tpa})_2]^{4+}$ (**5**) can also be obtained from chemical oxidation of **1a** with two equivalents of silver nitrate. Thus a solution of **1a** in acetone/water was reacted with two equivalents of silver nitrate, giving rise to rapid colour change from deep red to an intense blue solution. Addition of excess sodium hexafluorophosphate to the blue solution caused precipitation of the oxidized product $[\text{Co}_2(\text{bhnq})(\text{tpa})_2](\text{PF}_6)_4$ (**5b**), which was recrystallized from acetone/diethyl ether to give single crystals of **5b**·3Me₂CO in 30 % yield. Attempts to carry out a one-electron oxidation using one equivalent of silver nitrate did not yield any crystalline products.

The reaction of cobalt(II) perchlorate, $(\text{H}_3\text{tpa})(\text{ClO}_4)_3$, **bhnqH₂** and triethylamine in warm methanol affords red crystals of a salt of a new dinuclear cobalt(III) complex $[\text{Co}_2(\text{bhMenaph})(\text{tpa})_2]^{2+}$ (**6**) (**bhMenaph⁴⁻** is the tetraanionic form of bis-3,4-dihydroxy-4-methoxynaphthalene-1-one), which was identified crystallographically as $[\text{Co}_2(\text{bhMenaph})(\text{tpa})_2](\text{PF}_6)_2 \cdot 3\text{MeOH} \cdot 2\text{H}_2\text{O}$ (**6a**·3MeOH·2H₂O). It is likely that formation of the new ligand occurs *via* the metal catalysed reaction of **bhnq²⁻** with methoxide formed following deprotonation by triethylamine (Scheme 2, top). This procedure involves formal two-electron reduction of the organic ligand, with charge balance maintained by the accompanying oxidation of both cobalt centres to the trivalent state. While the one-electron reduction of quinones in the presence of hydroxide or alkoxide anions such as methoxide has been reported previously,³⁶⁻⁴⁰ there are no reports of a metal complex analogous to **6**, obtained from the *in situ* reduction of a quinone ligand. Reproducible microanalytical data measured on the solid sample of **6a** obtained from methanol/water indicate impurities that proved impossible to remove due to the poor solubility of **6a** in most solvents.

Scheme 2



The report of reduction of hmqH at high pH, leading to the isolation of the one-electron reduced radical form,⁴¹ prompted an exploration of the chemistry of **5** in strong base in an effort to obtain a dinuclear cobalt(III) complex with a reduced form of the bhnq ligand. Thus, treatment of a blue solution of **5b** in acetone with 5 M sodium hydroxide resulted in the formation of a deep red solution and ultimately a small quantity of red crystals of $[\text{Co}_2(\text{bhPronaph})(\text{tpa})_2](\text{PF}_6)_2$ (**7a**), where bhPronaph^{4-} is a tetraanionic form of bis-3,4-dihydroxy-4-(2-oxopropyl)naphthalen-1(4H)-one (Scheme 2, bottom). Although crystals of **7a** could be hand-picked for a partial structure determination

by single crystal X-ray diffraction (see below), it was not possible to obtain a bulk sample of **7a** or any other salt of $[\text{Co}_2(\text{bhPronaph})(\text{tpa})_2]^{2+}$ (**7**) for other physical measurements. As in the formation of **6**, the bhnq^{2-} ligand in **5** is transformed into the derivative bhPronaph^{4-} , facilitated by the hydroxide ions activating acetone to form an enolate, which attacks the carbonyl bound to the cobalt centre. In this case there is no change in the oxidation state of the cobalt centres, which remain cobalt(III).

A small quantity of crystals of the free ligand for X-ray diffraction analysis were obtained in the form $(\text{pyH})(\text{bhnqH})\cdot 2\text{H}_2\text{O}$ following dissolution of bhnqH_2 in pyridine.

Structure descriptions

The single crystal X-ray diffraction data for compounds **1b** $\cdot 2\text{CH}_2\text{Cl}_2\cdot 2\text{MeOH}$, **2a** $\cdot 2\text{MeCN}\cdot 2\text{Et}_2\text{O}$, **3a** $\cdot 2\text{MeCN}\cdot \text{H}_2\text{O}$, **4a** $\cdot 2\text{MeCN}\cdot 0.5\text{Et}_2\text{O}$, **5b** $\cdot 3\text{Me}_2\text{CO}$, **6a** $\cdot 3\text{MeOH}\cdot 2\text{H}_2\text{O}$, and $(\text{pyH})(\text{bhnqH})\cdot 2\text{H}_2\text{O}$ are available in Table 1. The crystals obtained for **7a** were only weakly diffracting and failed to provide high resolution reflection data. As a consequence only a partial structure determination was possible. Whilst the quality structure of the structure determination impacts upon the accuracy of the bond lengths and angles the atoms of complex **7** are clearly and unambiguously defined. Structural representations of complexes **1** in **1b** $\cdot 2\text{CH}_2\text{Cl}_2\cdot 2\text{MeOH}$, **5** in **5b** $\cdot 3\text{Me}_2\text{CO}$, **6** in **6a** $\cdot 3\text{MeOH}\cdot 2\text{H}_2\text{O}$ and **7** in **7a** are presented in Figure 1, while **2** in **2a** $\cdot 2\text{MeCN}\cdot 2\text{Et}_2\text{O}$, **3** in **3a** $\cdot 2\text{MeCN}\cdot \text{H}_2\text{O}$, **4** in **4a** $\cdot 2\text{MeCN}\cdot 0.5\text{Et}_2\text{O}$ and bhnqH^- in $(\text{pyH})(\text{bhnqH})\cdot 2\text{H}_2\text{O}$ are presented in Figure S1. Selected interatomic distances and angles are provided in Table 2.

Table 1. Crystal data for compounds **1b**·2CH₂Cl₂·2MeOH, **2a**·2MeCN·2Et₂O, **3a**·2MeCN·H₂O, **4a**·2MeCN·Et₂O, **5b**·3Me₂CO, **6a**·3MeOH·3H₂O and (pyH)(bhnqH)·2H₂O.

	1b ·2CH ₂ Cl ₂ ·2MeOH	2a ·2MeCN ·2Et ₂ O	3a ·2MeCN·H ₂ O	4a ·2MeCN·Et ₂ O	5b ·3Me ₂ CO	6a ·3MeOH·3H ₂ O	(pyH)(bhnqH) ·2H ₂ O
Empirical formula	C ₁₀₈ H ₉₆ B ₂ Cl ₄ Co ₂ N ₈ O ₈	C ₇₀ H ₇₄ Cl ₂ Co ₂ N ₁₀ O ₁₆	C ₆₄ H ₆₀ Cl ₂ Co ₂ N ₁₀ O ₁₅	C ₇₀ H ₇₂ Cl ₂ Co ₂ N ₁₀ O ₁₅	C ₆₅ H ₆₂ Co ₂ F ₂₄ N ₈ O	C ₅₉ H ₆₀ Co ₂ F ₁₂ N ₈ O	C ₅₀ H ₃₆ N ₂ O ₁₅
Formula weight /g mol ⁻¹	1915.21	1500.15	1397.98	1482.14	1796.97	1527.02	902.79
Temperature / K	130(2)	130(2)	130(2)	130(2)	130(2)	130(2)	130(2)
Crystal system	Triclinic	Monoclinic	Orthorhombic	Monoclinic	Monoclinic	Monoclinic	Triclinic
Space group	<i>P</i> -1	<i>C</i> 2/ <i>c</i>	<i>C</i> 222 ₁	<i>P</i> 2 ₁ / <i>c</i>	<i>P</i> 2 ₁ / <i>c</i>	<i>P</i> 2 ₁ / <i>n</i>	<i>P</i> -1
<i>a</i> / Å	9.6851(3)	34.0656(6)	8.8275(4)	19.0266(16)	16.9097(4)	17.577(4)	7.277(2)
<i>b</i> / Å	20.5451(5)	8.53010(10)	37.7023(17)	18.3969(15)	32.8461(8)	15.479(4)	11.987(3)
<i>c</i> / Å	22.8542(7)	25.9872(4)	18.6602(9)	20.8598(19)	13.4958(3)	22.795(5)	12.828(3)
<i>α</i> /°	85.949(2)	90	90	90	90	90	68.347(4)
<i>β</i> /°	87.043(2)	105.875(2)	90	106.282(9)	100.386(2)	97.642(6)	81.383(4)
<i>γ</i> /°	81.098(2)	90	90	90	90	90	76.412(4)
<i>V</i> /Å ³	4477.7(2)	7263.43(19)	6210.4(5)	7008.7(10)	7373.0(3)	6147(3)	1008.4(4)
<i>Z</i>	2	4	4	4	4	4	1
<i>ρ</i> _{calc} /mg m ⁻³	1.420	1.372	1.495	1.405	1.619	1.600	1.490
<i>μ</i> / mm ⁻¹	4.530	4.871	5.613	5.017	5.440	0.698	0.111
<i>F</i> [000]	1992	3120	2888	3080	3640	3032	470

2 θ range / $^{\circ}$	2.83 to 44.94	3.54 to 73.95	3.33 to 61.51	3.26 to 75.55	2.69 to 49.99	1.38 to 27.55	1.71 to 25.03
reflns measd	15937	26771	8076	27447	15353	38443	5325
unique reflns	6946	7277	4579	14094	7172	14015	3493
Data / restraints / parameters	6946 / 0 / 1128	7277 / 0 / 452	4579 / 10 / 412	14094 / 36 / 853	7172 / 24 / 1018	14015 / 6 / 825	3493 / 0 / 319
R_{int}	0.0239	0.0582	0.0617	0.0639	0.0498	0.0770	0.0960
Flack parameter			0.019(12)				
$R_1 [I > 2\sigma(I)]$	0.0465	0.0657	0.0915	0.0849	0.0871	0.0877	0.0744
wR_2 (all data)	0.1154	0.1776	0.2381	0.2350	0.1850	0.2634	0.2009
Goodness-of-fit F^2	1.058	1.052	1.100	1.027	1.149	0.982	1.136
$\Delta\rho_{\text{max,min}} / e \text{ \AA}^{-3}$	0.526 and -0.442	1.277 and -0.594	0.761 to -0.712	1.151 to -1.150	0.880 to -0.858	0.832 and -1.151	0.433 and -0.412

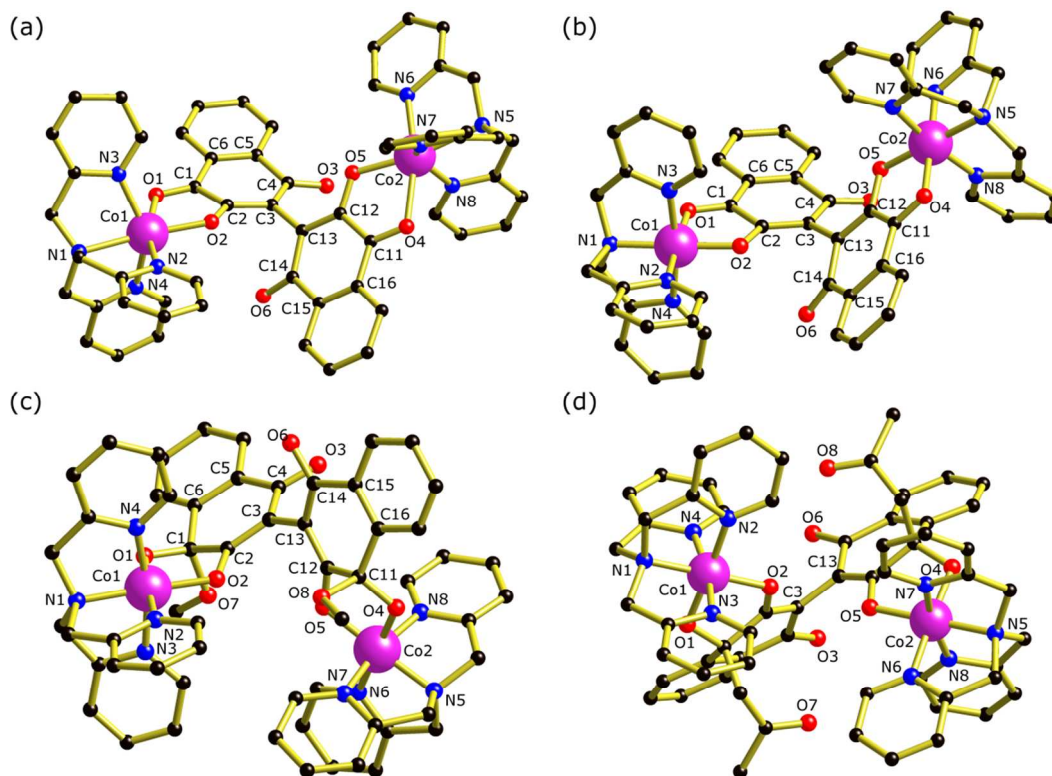


Figure 1. Structural representations of complexes (a) **1** in **1b**·2CH₂Cl₂·2MeOH, (b) **5** in **5b**·3Me₂CO, (c) **6** in **6a**·3MeOH·2H₂O and (d) **7** in **7a**.

Table 2. Selected interatomic distances and angles for complexes **1** in **1b**·2CH₂Cl₂·2MeOH, **2** in **2a**·2MeCN·2Et₂O, **3** in **3a**·2MeCN·H₂O, **4** in **4a**·2MeCN·Et₂O, **5** in **5b**·3Me₂CO, **6** in **6a**·3MeOH·3H₂O and (pyH)(bhnqH)·2H₂O

	1	2	3	4	5	6	bhnqH ⁻
Distances /Å							
Co···Co ^a	8.4858(12)	8.2469(10)	8.198(3)	8.1257(10)	8.027(2)	6.397(2)	-
Co-O	1.986(4)- 2.373(4)	1.990(2)- 2.162(2)	1.981(7)- 2.244(7)	1.985(2)-2.182(3)	1.857(7)- 1.929(6)	1.863(4)- 1.903(4)	-
Co-N ^b	2.233(4)- 2.264(4)	2.158(3)	2.128(8)	2.118(3)-2.132(4)	1.922(9)- 1.935(8)	1.921(4)- 1.965(5)	-
Co-N ^c	2.079(4)- 2.096(5)	2.090(3)- 2.164(3)	2.130(9)- 2.144(8)	2.136(3)-2.279(3)	1.894(8)- 1.922(9)	1.909(6)- 1.938(5)	-

O1-C1 (O4-	1.221(6)-	1.233(4)	1.237(12)	1.241(4)-1.246(4)	1.250(11)-	1.348(7)-	1.224(3)-
C11)	1.223(6)				1.258(11)	1.354(6)	1.225(3)
O2-C2 (O5-	1.270(6)-	1.294(4)	1.310(12)	1.290(4)-1.290(4)	1.317(11)-	1.301(6)-	1.295(3)-
C12)	1.294(6)				1.326(11)	1.303(6)	1.332(3)
O3-C4 (O6-	1.236(6)-	1.226(4)	1.230(12)	1.224(4)-1.238(4)	1.207(12)-	1.226(7)-	1.228(3)-
C14)	1.237(6)				1.235(12)	1.244(6)	1.231(3)
C1-C2 (C11-	1.492(8)-	1.503(5)	1.502(13)	1.503(4)-1.503(4)	1.474(14)-	1.513(7)-	1.493(4)-
C12)	1.509(7)				1.491(14)	1.513(8)	1.504(4)
C3-C13 (C3-	1.482(7)	1.482(6)	1.48(2)	1.469(4)	1.485(13)	1.479(7)	1.472(4)
C3')							
Angles /°							
Dihedral	137.16(10)	124.91(8)	128.1(2)	130.48(6)	131.1(2)	49.04(13)	42.87(4)
angle ^d							

^a Intramolecular distance between the cobalt centers. ^b Tertiary amine N atoms of the Me_ntpa ligand (*n* = 0-3). ^c Imine N atoms of the Me_ntpa ligand (*n* = 0-3). ^d The angle between the two planes as defined by carbon atoms C1-C10 and C1'-C10' (C11-C20).

The compound (pyH)(bhnqH)·2H₂O crystallises in the triclinic space group $P\bar{1}$ with one bis-naphthoquinone molecule, one pyridinium cation and two water molecules in the asymmetric unit. The crystal data at 130 K reveal the relatively short O1-C1 and O4-C11 (both 1.225(3) Å) distances, longer O2-C2 (1.332(4) Å) and O5-C12 (1.295(3) Å) distances and C1-C2 (C11-C12) bonds of both *o*-dioxolene sites in the range 1.492(4)-1.504(4) Å (Figure S1). The longer O2-C2 and shorter O5-C12 distances suggest the monoprotonated monoanionic bhnqH⁻ species. Bond valence sum calculations for these distances consistent with direct protonation of O2 only and a nearby region of electron density in the Fourier difference map is assigned this proton.⁴² Pyridinium atom N1 is similarly observed as protonated. Atom O5 interacts with the pyridinium cation through a NH···O hydrogen

bond with an N \cdots O distance of 2.629(3) Å, while an OH \cdots O hydrogen bond with an O \cdots O distance of 2.515(3) Å is also evident between O2 and O5.

Compounds **2a**·2MeCN·2Et₂O and **4a**·2MeCN·Et₂O crystallise in the monoclinic space groups *C2/c* and *P2₁/c*, respectively, while compounds **1b**·2CH₂Cl₂·2MeOH and **3a**·2MeCN·H₂O crystallise in the triclinic and orthorhombic space groups *P*-1 and *C222₁*, respectively. The respective asymmetric units contain the full dinuclear complexes **1** and **4** and half the complexes **2** and **3**, in addition to counteranions and solvent molecules. The dinuclear cobalt complexes **1-4** involve bhnq²⁻ ligands bridging two cobalt centres through oxygen donor atoms, with the coordination sphere of each cobalt centre completed by the nitrogen atoms of the capping Me_{*n*}tpa ligands (Figures 1 and S1). Each cobalt centre is 6-coordinate with distorted octahedral coordination geometry. The Co-O and Co-N bond lengths are in the respective ranges 1.981(7)-2.373(4) and 2.079(4)-2.279(3) Å for the four complexes, consistent with high spin cobalt(II) centres. Consideration of the O-C and (O)C-C(O) bond lengths provides information about the redox state of the bhnq ligand. The observed O1-C1 (O4-C11), O2-C2 (O5-C12), O3-C4 (O6-C14) and C1-C2 (C11-C12) distances for the four complexes fall in the ranges 1.221(6)-1.247(4), 1.270(6)-1.310(12), 1.226(4)-1.238(4) and 1.492(8)-1.509(7) Å, respectively. These data are consistent with the assignment of the dianionic state of the ligand that is present in all previously reported complexes.^{30-32,42,43}

Families of analogous cobalt complexes with Me_{*n*}tpa ligands for which all four members have been structurally characterised are relatively rare. Complexes **1-4** represent the first such family in which all four members possess cobalt(II) centres, which is in contrast to the previously reported [Co(CO₃)(Me_{*n*}tpa)]⁺ family that exhibits the cobalt(III) oxidation state for all four members.⁴⁴ As alluded to above, the tpa and Metpa analogues of the [Co(3,5-dbdiox)(Me_{*n*}tpa)] family involve cobalt(III) centres, while the Me₃tpa analogue displays a cobalt(II) centre and the Me₂tpa species undergoes a thermally-induced valence tautomeric transition from cobalt(III)-catecholate to cobalt(II)-

semiquinonate.³⁵ From Table 2, it is apparent that the increasing substitution of the Me_ntpa ligands affects the Co-N bond distances, with the distance to the tertiary amine nitrogen decreasing monotonically with increasing substitution, while the distances to the imine nitrogen atoms increase in the same range. A similar trend in the distance to the imine nitrogen atoms was observed for the cobalt(III) [Co(O₂CO)(Me_ntpa)]⁺ family, although there was little variation in the distance to the tertiary amine nitrogen in that case. In both cases the increasing steric demands as the ligand becomes more highly substituted leads to the observed Co-N bond lengthening.

Compounds **5b**·3Me₂CO, **6a**·MeOH·3H₂O and **7a** crystallise in the monoclinic space groups *P2₁/c*, *P2₁/n* and *P2₁/n*, respectively with the full dinuclear complexes present in the asymmetric unit. Complexes **5-7** again possess pairs of cobalt centres capped by tetradentate tpa ligands and bridged by bhmq²⁻, or its derivatives bhMenaph⁴⁻ and bhPronaph⁴⁻ (Figure 1). However, for complexes **5** and **6** the Co-O and Co-N bond lengths are in the respective ranges 1.848(8)-1.929(6) and 1.894(8)-1.965(5) Å, suggesting low spin cobalt(III) centres in these two complexes. For complex **5** the O1-C1 (O4-C11), O2-C2 (O5-C12), O3-C4 (O6-C14) and C1-C2 (C11-C12) ligand bond distances are similar to the equivalent distances in complexes **1-4**, generally varying by less than 0.03 Å. These data are consistent with retention of the bhmq²⁻ redox state in **5**, with the small differences attributable to the effect of the change in Co-O distances for di- versus trivalent cobalt.

An important structural feature of **6** and **7** is the presence of methoxy or oxopropyl groups in bhMenaph and bhPronaph, respectively. The bond lengths observed for bhMenaph⁴⁻ in **6** are comparable to the equivalent distances measured for some closely related organic compounds, such as 2-(2,5-dimethoxybenzene)-4,4,5-trimethoxy-cyclohexa-2,5-dienone, 2,6-di-*tert*-butyl-4,4,8-trimethoxy-1-oxo-1,4-dihydrodibenzofuran and 3-hydroxy-4,4,6-trimethoxy-2,5-di(*p*-methoxyphenyl)-cyclohexa-2,5-dien-1-one.⁴⁶⁻⁴⁸ The structure of bhPronaph⁴⁻ in complex **7** is comparable with those

reported for alkyl-substituted quinone compounds such as sarcodifurine A, chaetoinidicin B and azamerone.⁴⁹⁻⁵¹

The two halves of bhnq-derived ligands in (pyH)(bhnqH)·2H₂O and complexes **1-7** are not coplanar (Figure S2). The pertinent angle is the dihedral angle between the two naphthoquinone planes defined by carbon atoms C1-C10 and C1'-C10' (C11-C20). In (pyH)(bhnqH)·2H₂O, the dihedral angle of 42.87(4)° may be due to the close proximity of O2 and O5 and O3 and O6 with rotation about the C3-C13 (C3-C3') axis minimizing the steric hindrance between O2...O5 and O3...O6. The dihedral angles for **1-5** are in the range 124.91(8)-137.16(10)°, while the angle for **6** is 49.04(13)°. These are comparable with literature dihedral angles for bhnq²⁻ complexes in the range 50-118°. ³⁰⁻³³ The presence of the bulky Me_ntpa ligands in **1-7** likely leads to larger dihedral angles to satisfy the steric requirements of these complexes in the crystal lattice. Thus, the possibility of rotation around the C3-C13 (C3-C3') axis of the bhnq ligand family provides considerable structural flexibility in response to steric and packing effects.

Infrared spectroscopy

The infrared spectra of bhnqH₂ and compounds **1b**, **2a**, **3a**, **4a** and **5b** were acquired as pressed KBr disks. Comparison with spectra reported previously for transition metal complexes of hnqH has facilitated spectral assignment.^{18,22-24,26} For bhnqH₂, a broad absorption band at 3290 cm⁻¹ not apparent for the cobalt complexes, is assigned to the ν(O-H) vibrations of the phenol group. Bands between 1600 and 1700 cm⁻¹ are due to ν(C=O) vibrations, with the spectrum of bhnqH₂ showing two strong absorptions at 1673 and 1643 cm⁻¹ for the asymmetric and symmetric modes, respectively, as observed for other naphthoquinone systems. Upon coordination, both bands shift to lower wavenumbers by 30-40 cm⁻¹. The ν(C=C) vibrations are observed at 1590 cm⁻¹ for bhnqH₂, with bands evident at similar

frequencies for compounds **1b**, **2a**, **3a**, **4a** and **5b**, in addition to new bands at around 1540 cm^{-1} . Bands evident at around 1270 and $1215\text{-}1230\text{ cm}^{-1}$ are assigned to $\nu(\text{C-O})$ stretches.

Magnetic measurements

Variable temperature magnetic susceptibility data were obtained for powdered microcrystalline samples of compounds **3a**· $2\text{H}_2\text{O}$, **4a** and **5b**· Me_2CO in the temperature range $2\text{-}300\text{ K}$ (Figures 2 and S2). Unfortunately it was not possible to measure reliable data for **1a** or **1b** due to difficulties in obtaining pure bulk samples.

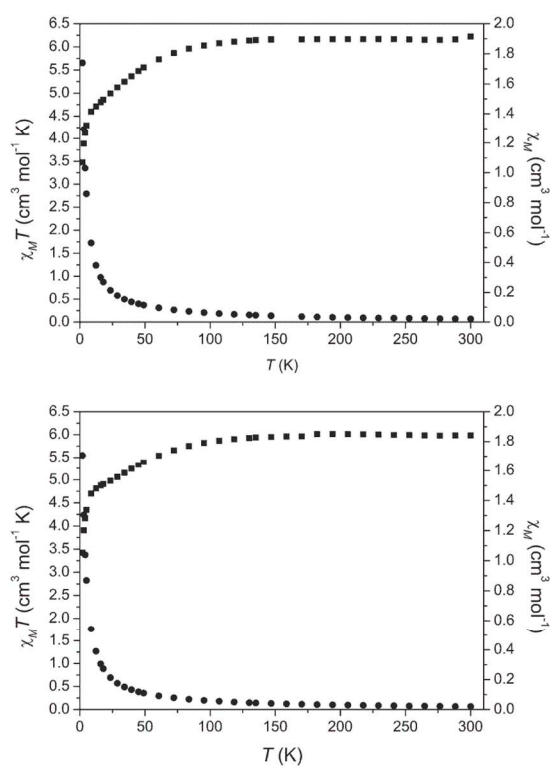


Figure 2. Magnetic susceptibility data measured for compounds **3a**· $2\text{H}_2\text{O}$ (top) and **4a** (bottom), plotted as χ_M (●) and $\chi_M T$ (■).

Compounds **3a**·2H₂O and **4a** display near identical thermal susceptibility profiles (Figure 2). Essentially temperature invariant $\chi_M T$ values of 6.1 and 6.0 cm³ mol⁻¹ K are evident in the temperature range 120-300 K for **3a**·2H₂O and **4a**, respectively. These $\chi_M T$ values are higher than the spin-only value of 3.75 cm³ mol⁻¹ K calculated for two non-interacting high spin cobalt(II) ions ($S = 3/2$, ${}^4T_{1g}$, $g = 2.0$). This is typical for distorted high-spin octahedral cobalt(II) ions due to the contribution of first order orbital angular momentum, with the ${}^4T_{1g}$ ground term split into six Kramers doublets by the combined effects of distortion of the octahedral crystal field and spin-orbit coupling.⁵² Below 120 K the data decrease gradually to a value of 4.8 cm³ mol⁻¹ K at 20 K, before a sharper decrease to 3.4 cm³ mol⁻¹ K at 2 K. The decrease observed in $\chi_M T$ upon cooling below 120 K is likely due to weak antiferromagnetic intramolecular exchange interactions between the two cobalt(II) centres, however the orbital contribution hinders a quantitative analysis of the data. The absence of a maximum in the plots of χ_M versus T are consistent with very weak coupling.⁵³ The sharper decrease below 20 K may be due to depopulation of the crystal field split energy levels (zero field splitting) and/or antiferromagnetic intermolecular interactions. It is possible, though unlikely, that the decrease in $\chi_M T$ upon cooling might be due to an incomplete spin crossover transition to low spin cobalt(II), as although spin crossover for cobalt complexes most commonly requires an N₆ coordination sphere, an example with an N₄O₂ coordination sphere has been reported.⁵⁴ A valence tautomeric cooling-induced transition from a Co(II)-bhnq²⁻-Co(II) species to a Co(III)-bhnq³⁻-Co(II) redox isomer is also a possibility, although the related mononuclear cobalt(II) complexes [Co(hnq)₂(NL)₂] and [Co(hnq)₂(N₂L)] show no sign of such a transition.²⁹

Although there are literature reports of polynuclear complexes of divalent manganese, cobalt, nickel and copper bridged by bhnq²⁻,³⁰⁻³³ no magnetic data are available for any complex in which bhnq²⁻ binds in a manner similar to that observed herein. Instead magnetic data have been reported for the trinuclear helical complex [Mn₃(bhnq)₃(H₂O)₂]·10.5H₂O,³³ in which three bhnq²⁻ ligands provide

μ_2 -aryloxo bridges that directly link manganese(II) centres. In this complex the antiferromagnetic Mn-O-Mn exchange interaction has been evaluated to be -0.75 cm^{-1} . Given this information, and the relatively large intramolecular cobalt...cobalt separations of more than 8 \AA , it is likely that any magnetic coupling in **3** and **4** is small. It is however, reasonable to assume that the overlap of magnetic orbitals of paramagnetic centres bridged by bhnq^{2-} , and therefore any magnetic coupling, will depend on the dihedral angle of the ligand hinge.

The data for **5b** $\cdot 3\text{Me}_2\text{CO}$ (Figure S3) indicate the sample is diamagnetic, as expected for low spin cobalt(III) with a diamagnetic bhnq^{2-} ligand, with the temperature independent paramagnetism that is typically observed for cobalt(III) also in evidence.⁵⁵ Although a valence tautomeric transition from $\text{Co(III)-bhnq}^{2-}\text{-Co(III)}$ to a $\text{Co(II)-bhnq}^-\text{-Co(III)}$ species might be anticipated upon heating from the 130 K used for the X-ray diffraction study, this was not observed up to 300 K. Spin crossover transitions are not expected for cobalt(III) complexes.

Electronic spectroscopy

The room temperature UV-visible absorption spectra were measured for acetonitrile solutions of compounds **1a**, **2a**, **3a**, **4a** and **5b** between 210 and 800 nm (Figure 3, Table S1). In each case, no spectral changes were evident over a period of three hours, indicating solution stability for this time period.

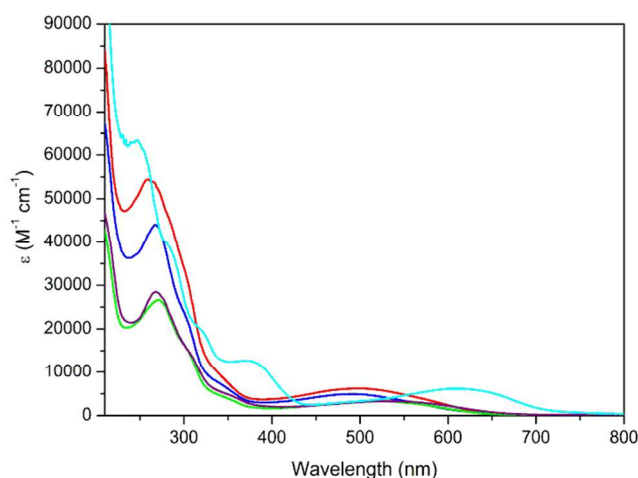


Figure 3. Electronic absorption spectra for **1a** (red), **2a** (blue), **3a** (green), **4a** (purple) and **5b** (cyan) in acetonitrile.

The spectra of compounds **1a-4a** all exhibit a sharp absorption band between 258 and 268 nm ($\epsilon = 2.8\text{-}5.4 \times 10^4 \text{ M}^{-1} \text{ cm}^{-1}$). This band is also observed for the free bhnq^{2-} (265 nm, $\epsilon = 2.7 \times 10^4 \text{ M}^{-1} \text{ cm}^{-1}$) and for the mononuclear cobalt(II) complex $[\text{Co}(\text{hnq})_2(\text{py})_2]$ and is assigned to the ligand $\pi \rightarrow \pi^*$ transition.²² A poorly resolved shoulder is evident between 320 and 350 nm, which is consistent with the shoulder assigned to the ligand $n \rightarrow \pi^*$ transition at 336 nm for $[\text{Co}^{\text{II}}(\text{hnq})_2(\text{py})_2]$.²² A broad asymmetric band observed for **1a-4a** between 481 and 537 nm ($\epsilon = 3.8\text{-}6.3 \times 10^3 \text{ M}^{-1} \text{ cm}^{-1}$) is also observed for $[\text{Cu}(\text{bhnq})(\text{X})_2]_n$ ($\text{X} = \text{H}_2\text{O}$ or THF) between 480–550 nm^{30,31} and is assigned as a metal to ligand charge transfer (MLCT) transition from cobalt(II) to the bhnq^{2-} ligand. This band appears to generally shift towards higher wavelength as the number of methyl groups in the 6-position of the capping Me_ntpa ligands increases. This is visually evident from the colour of the solutions, which change from dark red for **1a** to purple for **4a**.

The electronic absorption spectrum of the acetonitrile solution of the cobalt(III) compound **5b** differs to those of the cobalt(II) compounds **1a-4a** discussed above. The bhnq^{2-} $\pi \rightarrow \pi^*$ transition is again observed at 270 nm ($\epsilon = 4.1 \times 10^4 \text{ cm}^{-1} \text{ M}^{-1}$), with a broad band at 614 nm ($\epsilon = 6.1 \times 10^3 \text{ cm}^{-1} \text{ M}^{-1}$)

¹) and additional bands at 367 ($\epsilon = 1.2 \times 10^4 \text{ cm}^{-1} \text{ M}^{-1}$) and 325 ($\epsilon = 1.8 \times 10^4 \text{ cm}^{-1} \text{ M}^{-1}$). While UV-visible absorption spectra for trivalent metal complexes of hmq and bhmq ligands have not been reported, the spectra of the cobalt(III) complexes [Co(3,5-DBCat)(3,5-DBSQ)(2,2'-bipy)] and [Co₂(dhbq)(tpa)₂]³⁺ (3,5-DBCat = 3,5-di-*tert*-butylcatechol; 3,5-DBSQ = 3,5-di-*tert*-butyl-semiquinone; dhbq = 2,5-dihydroxy-1,4-benzoquinone in the catechol-semiquinone form) display absorption bands at 610 and 536 nm, respectively, which were attributed to ligand to metal charge transfer (LMCT) transitions for the catecholate-cobalt(III) chromophores.^{8,56} On this basis, the absorption at 614 nm for **5b** is assigned to an analogous LMCT band arising from the cobalt(III)-bhmq chromophore.

Electrochemistry

Cyclic voltammograms were measured for acetonitrile (1.0 mM) solutions of compounds **1a**, **2a**, **3a** and **4a** with 0.1 M (Bu₄N)(PF₆) as the supporting electrolyte. For comparison, voltammograms were also measured in the same medium for bhmqH₂ doubly deprotonated with two equivalents of triethylamine (Figure 4). These systems proved not amenable to steady state linear sweep voltammetry with a microelectrode, due to adsorption onto the electrode surface giving poor resolution for all processes. However the position of zero current in these measurements did confirm the processes as either reductions or oxidations. The measured oxidation (E_{pa}) and reduction (E_{pc}) peak potentials (E_p) from the cyclic voltammograms (100 mVs⁻¹ scan rate) are tabulated in Table 3, together with the mid-point potentials (E_m) and peak-to-peak separations (ΔE_p) for the quasi-reversible processes. All potentials are quoted versus the ferrocene/ferrocenium couple.

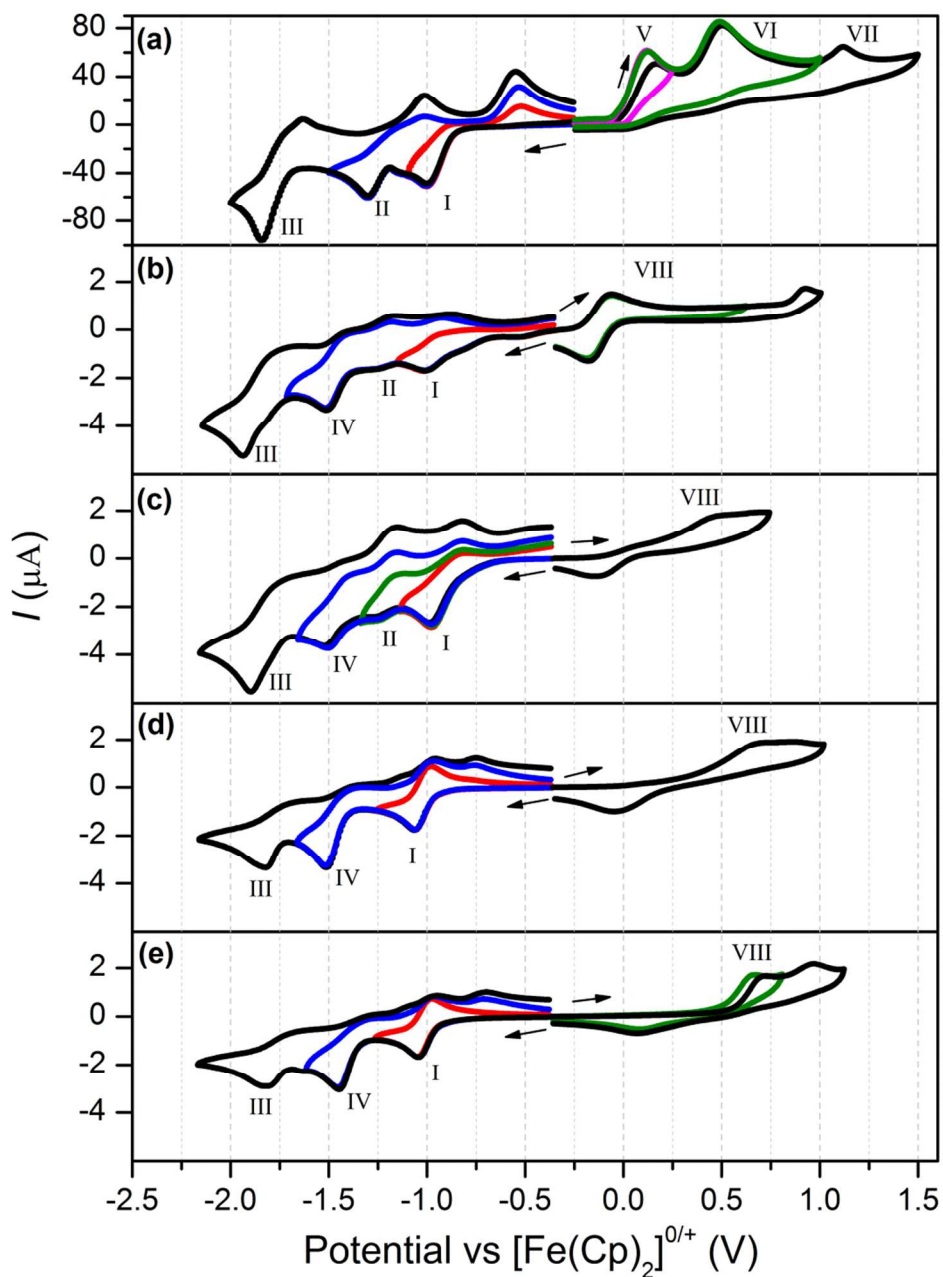


Figure 4. Cyclic voltammograms for (a) bhnq^{2-} , (b) **1a**, (c) **2a**, (d) **3a** and (e) **4a** (1.0 mM in acetonitrile with 0.1 M TBAPF_6) obtained with a 1 (b-d) or 3 (a) mm diameter glassy carbon electrode at a scan rate of 100 mV s^{-1} . The different coloured lines plot the voltammograms measured with different switching potentials to probe reversibility.

Table 3. E_p or E_m / V and (ΔE_p / mV) for compounds **1a**, **2a**, **3a** and **4a**.

Compound	E_p or E_m / V (ΔE_p / mV)							
	Reductions (E_{pc})				Oxidations (E_{pa})			
	III	IV	II	I	V	VIII	VI	VII
bhnq ²⁻	-1.84	-	-1.30	-1.02	0.122	-	0.50	1.12
1a	-1.94	-1.52	-1.25	-1.02	-	-0.125 (130) ^a	-	-
2a	-1.89	-1.52	-1.24	-0.888 (180) ^a	-	0.473	-	-
3a	-1.82	-1.51	-	-1.02 (75) ^a	-	0.690	-	-
4a	-1.82	-1.45	-	-1.01 (80) ^a	-	0.718	-	-

^a E_m ^b not evident in Figure 3

The cyclic voltammograms for deprotonated bhnq²⁻ (Figure 4a) exhibit three resolved reduction processes labelled I, II and III. These processes are not reversible, although oxidation processes are observed on the reverse scan. Electrochemical studies of hmq⁻ in DMSO reveal a quasi-reversible reduction to the radical hmq^{•2-} species, with an E_{pc} value of -1.79 V (500 mVs⁻¹ scan rate) versus ferrocene/ferrocenium.²² Detailed studies suggest this process is proton-coupled and this is likely also the case for the equivalent processes for bhnq²⁻, although the media in which the compounds were measured differs. Indeed the voltammetric response associated with process I is characteristic for a fast chemical step following reduction, with the reduction likely proton-coupled, leading to the observed chemical irreversibility. On scanning to positive potentials three irreversible oxidation processes are also observed for bhnq⁻, labelled V, VI and VII, while for hmq⁻ a comparable oxidative process was apparent on the published voltammogram, with an E_{pa} of around 0.4 V.²² This presumably involves oxidation to the neutral radical hmq[•] species. The voltammetric behaviour

measured for bhnq^- is complicated and it is not possible to elucidate the numbers of electrons and protons associated with the observed processes for bhnq^{2-} . However the free ligand is certainly redox-active with both oxidative and reductive processes apparent at relatively accessible potentials.

Upon scanning in the negative direction, the cyclic voltammograms (Figure 4b-e) for compounds **1a**, **2a**, **3a** and **4a** reveal up to four processes (labelled I, II, III, IV). The position of zero current in the steady-state voltammograms confirmed the assignment of these processes as reductions. For comparison a solution of the complex $[\text{Co}^{\text{II}}(\text{hnq})_2(\text{py})_2]$ in DMSO displays two quasi-reversible reductions, assigned as ligand-based, with E_{pc} values of -1.20 and -1.84 V (100 mVs^{-1} scan rate) versus ferrocene/ferrocenium.²² The voltammograms of compounds **1a** and **2a** exhibit four reductive processes, three of which (I, II and III) appear to correspond to the processes observed for free bhnq^{2-} , with slight shifts to more negative potentials. A new reductive process (labelled IV) is also apparent with an E_{pc} of -1.5 V, which is tentatively assigned to reduction of cobalt(II) to cobalt(I).⁵⁷ The voltammograms measured for **3a** and **4a** are a little different, with process II no longer apparent and process IV of increased intensity and shifted to more positive potentials. This is perhaps due to overlap of ligand- and metal-based reductions in these compounds. In addition, for **3a** and **4a** process I displays quasi-reversibility, with the ratios of anodic and cathodic currents approaching unity and ΔE_p values of 75 and 80 mV when the potential is switched before the next process.

The voltammograms acquired in the oxidative region for compounds **1a**, **2a**, **3a** and **4a** reveal one or two processes labelled VIII and V. For compound **1a** process VIII shows quasi-reversibility with the ratio of anodic and cathodic currents approaching unity and a ΔE_p value of 130 mV. Process VIII shifts monotonically to more positive potentials as the number of methyl substituents on the Me_ntpa ancillary ligands increases from none in **1a** to four in **3a**. This suggests that this process is associated with oxidation from cobalt(II) to cobalt(III). A similar shift was observed previously for the $[\text{Co}_2(\text{spiro})(\text{Me}_n\text{tpa})_2]^{2+}$ family of dinuclear complexes,¹³ as well as for families of mononuclear

copper and cobalt complexes with Me_ntpa ligands.^{35,58} This shift directly reflects the steric influence of the methyl substituents of the Me_ntpa ligand on the Co-O/N bond lengths, and therefore the ease of oxidation to the smaller cobalt(III). The shift in the potential for oxidation of cobalt(II) also correlates with the relative ease of chemically oxidising complex **1** to obtain the cobalt(III) complex **5**, while similar attempts to chemically oxidise the Me_ntpa ($n = 2-4$) complexes **2-4** were unsuccessful. Interestingly, the degree of chemical reversibility of process VIII varies across the four complexes, as it does for the $[\text{Co}_2(\text{spiro})(\text{Me}_n\text{tpa})_2]^{2+}$ family, although the origin of this is not known. The remaining oxidation, process V, is irreversible, with E_p values that vary little between compounds **1a-4a**, suggesting that it is ligand rather than metal-based.

Concluding remarks

This study has explored several aspects of the chemistry of dinuclear cobalt complexes with the bhnq^{2-} family of ligands. Systematic derivatisation of the Me_ntpa ancillary ligands has revealed that the oxidation of cobalt(II) to cobalt(III) becomes less favourable upon increasing substitution of the Me_ntpa ligand. In the related $[\text{Co}_2(\text{spiro})(\text{Me}_n\text{tpa})_2]^{2+}$ family of complexes that we reported recently, the equivalent trend led to the ligand and metal-based redox processes switching relative potentials between the Me_1tpa and Me_2tpa analogues.¹³ This gave rise to both Co(III)-catecholate and Co(II)-semiquinonate charge distributions across the four complexes in the family and a valence tautomeric transition for the $[\text{Co}_2(\text{spiro})(\text{Me}_2\text{tpa})_2]^{2+}$ analogue. However, no such switch in redox potential is observed for the $[\text{Co}_2(\text{bhnq})(\text{Me}_n\text{tpa})_2]^{2+}$ family, with all four analogues exhibiting the Co(II)- bhnq^{2-} -Co(II) charge distribution. Given this room temperature charge distribution for all four complexes, the most likely candidate for a cooling-induced valence tautomeric transition to Co(III)- bhnq^{3-} -Co(II) redox isomer is the species with ligand and metal-based redox processes closest together in potential, as the potential difference corresponds to the energy separation of the relevant metal and ligand-based

frontier orbitals. In the family reported herein this is the $[\text{Co}_2(\text{bhnq})(\text{tpa})_2]^{2+}$ complex **1** and it is unfortunate that a pure bulk sample could not be obtained for variable temperature magnetic measurements.

Chemical oxidation of complex **1** affords the Co(III)- bhnq^{2-} -Co(III) complex **5**, $[\text{Co}_2(\text{bhnq})(\text{tpa})_2]^{4+}$, with oxidation having taken place at the cobalt centres in preference to the bhnq^{2-} ligand. Efforts to obtain analogous oxidised derivatives of the Me_ntpa ($n = 2-4$) complexes were unsuccessful, consistent with the more positive redox potentials observed voltammetrically for oxidation of the cobalt(II) centres. Exposure of the $[\text{Co}_2(\text{spiro})(\text{tpa})_2]^{2+}$ complex to either methoxide or acetone enolate ions gives rise to metal-catalysed derivatisation and formal reduction of the bhnq^{2-} ligand, with concomitant oxidation of the cobalt centres. Complexes **5**, **6** and **7** are the first complexes of bhnq^{2-} with trivalent, rather than divalent metal centres.

Experimental section

Synthesis

Unless indicated otherwise, all manipulations were performed under aerobic conditions using materials as received. Ligand bhnqH_2 was synthesized as described in the literature and no further purification was performed.¹⁴ The tris(2-pyridylmethyl)amine ligands $(\text{H}_3\text{tpa})(\text{ClO}_4)_3$, $(\text{H}_3\text{Metpa})(\text{ClO}_4)_3$, Me_2tpa and Me_3tpa were synthesised by literature methods using dichloromethane that was dried over CaH_2 .^{59,60}

$[\text{Co}_2(\text{bhnq})(\text{tpa})_2](\text{ClO}_4)_2$ (1a). Triethylamine (0.72 ml, 5.2 mmol) was added to a suspension of $(\text{H}_3\text{tpa})(\text{ClO}_4)_3$ (1.03 g, 1.73 mmol) in water until a clear solution was obtained. Solid $\text{Co}(\text{ClO}_4)_2 \cdot 6\text{H}_2\text{O}$ (0.63 g, 1.7 mmol) was then added to the solution which turned from colourless to deep green. A suspension of bhnqH_2 (0.30 g, 0.87 mmol) and triethylamine (0.24 ml, 3.5 mmol) in water (5 ml) was

added to the reaction mixture until a red precipitate was obtained. The temperature was then increased to 80° C and stirring was continued for further one hour. The resulting dark red solid was collected by filtration, washed with warm water and air dried to yield **1a** in 40% yield, although it was not possible to obtain an analytically pure sample. ESI-MS (MeCN) m/z : 694.5 $\{[\text{Co}(\text{bhnq})(\text{Htpa})]_2\text{H}\}^{2+}$, 522.4 $\{\text{Co}_2(\text{bhnq})(\text{Htpa})_2\}^{2+}$, 291.3 $\{\text{Htpa}\}^+$. Selected IR data (KBr, cm^{-1}): 3440 (m), 3069 (w), 1630 (m), 1610 (m), 1587 (s), 1536 (s), 1483 (w), 1439 (w), 1402 (m), 1355 (w), 1327 (w), 1273 (s), 1225 (w), 1087 (s), 1024 (w), 1003 (w), 798 (m), 738 (m), 623 (m), 504 (w), 420 (w).

$[\text{Co}_2(\text{bhnq})(\text{tpa})_2](\text{BPh}_4)$ (1b). Sodium borohydride (0.050 g, 1.3 mmol) was added in portions to a solution of **1a** (0.50 g, 0.40 mmol) in methanol (20 ml) until a pale red solution was obtained. Stirring was continued for a further 10 minutes affording a dark red solution. Addition of sodium tetraphenylborate (0.27 g, 0.80 mmol) to the solution afforded red microcrystals, which were then filtered and washed with methanol to afford **1b**. Recrystallisation from dichloromethane/methanol afforded dark red crystals of **1b**·2CH₂Cl₂·2MeOH. The crystals were washed and air dried, affording a partially desolvated sample of **1b**·CH₂Cl₂·2MeOH in 20% yield. A sample for crystallography was maintained in contact with mother liquor to prevent the loss of interstitial solvent. Anal. Calcd for **1b**·CH₂Cl₂·2MeOH; C₁₀₇H₉₄N₈Co₂O₈B₂Cl₂: C, 70.21; H, 5.18; N, 6.12%. Found: C, 69.83; H, 4.99; N, 6.30%. ESI-MS (MeCN) m/z : 694.5 $\{[\text{Co}(\text{bhnq})(\text{Htpa})]_2\text{H}\}^{2+}$, 522.4 $\{\text{Co}_2(\text{bhnq})(\text{Htpa})_2\}^{2+}$, 291.3 $\{\text{Htpa}\}^+$. Selected IR data (cm^{-1}) 3424 (m), 3054 (m), 3032 (m), 2998 (m), 2982 (m), 1635 (m), 1607 (m), 1588 (s), 1537 (s), 1480 (w), 1436 (w), 1397 (m), 1351 (w), 1325 (w), 1272 (s), 1225 (w), 1156 (w), 1053 (w), 1024 (w), 1004 (w), 791 (w), 734 (m), 706 (m), 612 (w), 423 (w).

Co₂(bhnq)(Metpa)₂](ClO₄)₂ (2a). An aqueous solution of (H₃MeTPA)(ClO₄)₃ (0.699 g, 0.577 mmol) and triethylamine (482 μl , 3.47 mmol) was added to an aqueous solution of Co(ClO₄)₂·6H₂O (0.422,

1.16 mmol) and stirred for 10 minutes, where the solution turned dark brown in colour. To this reaction mixture was added an aqueous suspension of bhnqH_2 (0.200 g, 0.577 mmol) and triethylamine (161 μl , 1.16 mmol), with a maroon microcrystalline precipitate forming over a period of 30 minutes. This precipitate was isolated by filtration and recrystallised by layering a concentrated acetonitrile solution with diethyl ether, to give dark purple rectangular plate crystals of $\mathbf{2a}\cdot 2\text{MeCN}\cdot 2\text{Et}_2\text{O}$. The product was isolated by filtration, washed with minimum mixture of acetonitrile/diethyl ether and air dried, affording a partially desolvated sample of $\mathbf{2a}\cdot 1.5\text{H}_2\text{O}$ in 54 % yield. A sample for crystallography was maintained in contact with mother liquor to prevent the loss of interstitial solvent. Anal. Calcd for $\mathbf{2a}\cdot 1.5\text{H}_2\text{O}$; $\text{C}_{58}\text{H}_{51}\text{N}_8\text{Cl}_2\text{Co}_2\text{O}_{15.5}$: C, 53.72; H, 3.96; N, 8.64, Cl 5.47. Found: C, 54.06; H, 3.92; N, 8.14; Cl, 5.80 %. Selected IR data (KBr, cm^{-1}): 3441 (s), 2919 (w), 2850 (w), 1710 (w), 1631 (m), 1608 (m), 1587 (m), 1540 (m), 1461 (w), 1442 (w), 1385 (w), 1352 (w), 1325 (w), 1273 (m), 1227 (w), 1160 (w), 1096 (m), 1007(w), 940 (w), 905 (w), 768 (w), 738 (w), 665 (w), 623 (w), 546 (w), 423 (w).

$[\text{Co}_2(\text{bhnq})(\text{Me}_2\text{tpa})_2](\text{ClO}_4)_2$ (**3a**). A methanol solution of Me_2tpa (0.552 g, 0.173 mmol) was added to a stirring methanol solution of $\text{Co}(\text{ClO}_4)_2\cdot 6\text{H}_2\text{O}$ (0.634 g, 1.173 mmol). Following 15 minutes of stirring, a mixture of bhnqH_2 (0.300 g, 0.866 mmol) and triethylamine (241 μl , 1.173 mmol) was added and stirred for approximately 30 minutes, which formed dark red precipitate. Following isolation of this solid by filtration, dark purple rectangular plate crystals of $\mathbf{3a}\cdot 2\text{MeCN}\cdot \text{H}_2\text{O}$ were formed by layering a concentrated acetonitrile solution with diethyl ether. The sample was washed with minimum amount of acetonitrile/diethyl ether and air-dried, affording $\mathbf{3a}\cdot 2\text{H}_2\text{O}$ in 39 % yield. A sample for crystallography was maintained in contact with mother liquor to prevent the loss of interstitial solvent. Anal. Calcd for $\mathbf{3a}\cdot 2\text{H}_2\text{O}$; $\text{C}_{60}\text{H}_{56}\text{N}_8\text{Cl}_2\text{Co}_2\text{O}_{16}$: C, 54.03; H, 4.23; N, 8.40, Cl 5.32. Found: C, 53.86; H, 4.24; N, 8.37; Cl, 5.24

%. Selected IR data (KBr, cm^{-1}): 3442 (s), 3070 (w), 2924 (m), 2854 (m), 1629 (m), 1608 (m), 1586 (m), 1541 (m), 1456 (m), 1395 (m), 1351 (m), 1326 (m), 1274 (m), 1227 (w), 1160 (w), 1096 (s), 1005 (w), 940 (w), 907 (w), 787 (w), 736 (w), 686 (w), 666 (w), 623 (w), 547 (w), 519 (w), 502 (w), 462 (w), 424 (w).

[Co₂(bhnq)(Me₃tpa)₂](ClO₄)₂ (4a). This complex was synthesised in a manner analogous to that employed for complex **3**, with the replacement of Me₂tpa with Me₃tpa to afford crystals of **4a**·2MeCN·0.5Et₂O. The product was isolated by filtration, washed with minimum amount of acetonitrile/diethyl ether and air dried, affording a desolvated sample of **4a** in 48 % yield. A sample for crystallography was maintained in contact with mother liquor to prevent the loss of interstitial solvent. Anal. Calcd for **4a**; C₆₂H₅₆N₈Cl₂Co₂O₁₄: C, 56.16; H, 4.26; N, 8.45, Cl 5.35. Found: C, 56.12; H, 4.35; N, 8.43; Cl, 5.42 %. Selected IR data (KBr, cm^{-1}): 3441 (s), 2922 (w), 2852 (w), 1630 (m), 1608 (m), 1587 (m), 1538 (w), 1456 (w), 1384 (w), 1350 (w), 1324 (w), 1299 (w), 1277 (w), 1228 (w), 1164 (w), 1095 (m), 1009 (w), 906 (w), 790 (w), 736 (w), 665 (w), 623 (w), 543 (w), 424 (w).

[Co₂(bhnq)(tpa)₂](ClO₄)₄ (5a). Solid **1a** (0.20 g, 0.16 mmol) was dissolved in methanol/acetone (10 ml, 1:1 mixture). Slow evaporation of the solution afforded crystals, which were isolated by filtration, washed with minimum amount of a diethyl ether and air dried, affording a partially hydrated sample of **5a**·4H₂O in 20% yield. Anal. Calcd for **5a**·4H₂O, C₅₆H₅₂N₈Co₂O₂₆Cl₄: C, 44.46; H, 3.46; N, 7.41%. Found: C, 44.41; H, 3.26; N, 7.38%. Selected IR data (cm^{-1}) 3441 (m), 3119 (w), 1628 (m), 1612 (m), 1540 (s), 1498 (m), 1462 (s), 1450 (s), 1393 (m), 1363 (s), 1269 (s), 1101 (s), 906 (m), 886 (m), 772 (s), 729 (s), 670 (m), 623 (s), 504 (w), 444 (w).

[Co₂(bhnq)(tpa)₂](PF₆)₄ (5b). To a stirred solution of **1a** (0.50 g, 0.40 mmol) in acetone/water (10 ml, 1:1 mixture) was added silver nitrate (0.14 g, 0.80 mmol) and the stirring continued until a blue purple solution was obtained. Potassium hexafluorophosphate (0.37 g, 2.0 mmol) was then added affording a dark grey precipitate. The material was collected by filtration and washed with diethyl ether. Recrystallisation was performed by dissolving the material in acetone and layered by diethyl ether to afford large red plate-like crystals. The crystals were collected by filtration, washed with diethyl ether and air dried to afford **5b**·3Me₂CO in 30% yield. A sample for crystallography was maintained in contact with mother liquor to prevent the loss of interstitial solvent. Anal. Calcd for **5b**·3Me₂CO, C₆₅H₆₂N₈Co₂O₉P₄F₂₄: C, 43.45; H, 3.48; N, 6.24%. Found: C, 43.29; H, 3.25; N, 5.97%. Selected IR data (cm⁻¹) : 3441 (m), 3119 (w), 1704 (w), 1630 (m), 1613 (m), 1542 (s), 1464 (m), 1364 (s), 1270 (s), 1166 (w), 839 (s), 769 (m), 729 (w), 671 (w), 558 (s), 504 (w), 444 (w).

[Co₂(bhMenaph)(tpa)₂](PF₆)₂ (6a). Triethylamine (0.72 ml, 5.2 mmol) was added to a suspension of (H₃tpa)(ClO₄)₃ (1.03 g, 1.73 mmol) in methanol (20 ml) until a clear solution was obtained. Solid Co(ClO₄)₂·6H₂O (0.63 g, 1.7 mmol) was then added to the solution which turned from colourless to deep green. A suspension of bhnqH₂ (0.30 g, 0.87 mmol) and triethylamine (0.24 ml, 3.5 mmol) in methanol (5 ml) was then added to the solution and the mixture was heated to 80 °C with stirring for 30 minutes. A suspension of sodium hexafluorophosphate (0.48 g, 2.6 mmol) in water (10 ml) was added to the hot solution and stirring was continued for further 15 minutes. Upon cooling to room temperature, the mixture was filtered to remove undissolved sodium salt and left stand for 2 days to afford red crystals. A sample for crystallography identified as **6a**·3MeOH·2H₂O was maintained in contact with mother liquor to prevent the loss of interstitial solvent. Although a single crystal could be hand-picked for X-ray diffraction analysis, it was not possible to obtain a pure bulk sample, with

elemental analysis indicating that the obtained samples of **6a** were contaminated with impurities, with further purification inhibited by the low solubility of **6a**.

[Co₂(bhPronaph)(tpa)₂](PF₆)₂ (7a). Concentrated sodium hydroxide (0.1 ml, 5 M) was added to a solution of **5b** (0.20 g, 0.16 mmol) in acetone and the mixture was shaken vigorously for 3 minutes. The deep red solution was then filtered and the filtrate was left stand for 5 days to afford a small quantity of crystals **7a**. A sample for crystallography was maintained in contact with mother liquor to prevent the loss of interstitial solvent. A single crystal was hand-picked for X-ray diffraction analysis, which allowed a partial structure determination.⁶¹ It was not possible to obtain a pure bulk sample for other measurements.

(pyH)(bhnqH). Dissolution of solid bhnqH₂ (0.20 g, 0.58 mol) in pyridine (3 ml) afforded a small quantity of orange crystals of (pyH)(bhnqH)·2H₂O within two days. One crystal was hand-picked for a single crystal X-ray analysis. ESI-MS (MeOH) *m/z*: 345.0 {Hbhnq}⁻. ¹H NMR (400 MHz, DMSO-*d*₆): δ 7.46 (m, 2H), 7.88 (m, 2H), 7.92 (m, 1H), 7.96 (d, 1H), 8.07 (d, 1H), 8.61 (s, 2H). ¹³C NMR (100 MHz, DMSO-*d*₆): δ 116.3, 125.9, 130.6, 132.4, 133.2, 149.2, 157.4, 181.3, 182.3.

X-ray diffraction

Data for **1b**·2CH₂Cl₂·2MeOH, **2a**·2MeCN·2Et₂O, **3a**·2MeCN·H₂O, **4a**·2MeCN·1/2Et₂O **5b**·3Me₂CO and **7a** were collected on an Oxford Xcalibur X-ray diffractometer fitted with CuKα radiation, while those for **6a**·3MeOH·2H₂O and (pyH)(bhnqH)·2H₂O were collected on a Bruker CCD X-ray diffractometer fitted with MoKα radiation. The crystals were transferred from the mother liquor to a protective oil to prevent potential solvent loss.

The structures were solved using direct methods within SHELXS.⁶² All data refinements were carried out using a least-squares method of F^2 with SHELXL-97. Anisotropic displacement parameters were applied to non hydrogen atoms except for the disordered atoms that are treated for partial occupancies. Semi empirical absorption correction was applied to the structures using SADABS and ABSPACK programs.^{63,64} The hydrogen atoms were placed in calculated positions and refined using a riding model. Most of the structures contain heavily disordered solvent molecules and the 'SQUEEZE' routine in PLATON was used to generate a modified HKL file that did not contain the contribution of the disordered solvent to the data.

Magnetic measurements

Variable temperature magnetic susceptibility measurements were performed with a Quantum Design MPMS-5 susceptometer, equipped with a 5 T magnet. Data were collected on powdered dried crystals, with the sets of susceptibility data collected at magnetic fields of 0.01, 0.1 and 0.5 T. Pascal's constants were used to estimate the diamagnetic correction for each complex.

Electrochemistry

Electrochemical measurements were performed in acetonitrile at 293 ± 2 K using a standard three electrode setup connected to an eDAQ computer-controlled potentiostat. Measurements were performed under a continuous nitrogen flow. The three-electrode system comprised of a 1.0 mm diameter glassy carbon (eDAQ) working electrode, a platinum wire auxiliary electrode and a commercially available Ag/AgCl reference electrode (eDAQ). Analyte solutions of 1.0 mM were prepared in acetonitrile containing 0.1 M $(\text{Bu}_4\text{N})(\text{PF}_6)$ as the supporting electrolyte. All potentials have been referenced versus the ferrocene/ferrocenium redox couple.

Other measurements

Infrared spectra were recorded as pressed KBr disks on a Bruker FTIR Tensor 27 spectrometer as pressed KBr disks. NMR spectra were recorded on a Varian Unity Plus 400 NMR spectrometer. ESI-MS spectra were performed on a Micromass Quattro II mass spectrometer in the positive ion mode for the metal complexes and in the negative ion mode for (pyH)(bhnqH). Electronic absorption spectra were measured on a Varian 50 Bio UV-Visible spectrophotometer 1 cm quartz cells. Elemental analyses were performed by the Microanalytical Unit, Research School of Chemistry, Australian National University, Australia.

Acknowledgements

We thank the Australian Research Council for funding.

Notes and references

^a School of Chemistry, University of Melbourne, Melbourne, 3010, Victoria, Australia. E-mail:

c.boskovic@unimelb.edu.au

^b School of Chemistry, Monash University, Clayton, Victoria, 3800, Australia

† Electronic Supplementary Information (ESI) available: additional structural representations, magnetic data and electronic absorption spectral data; hmq⁻ redox scheme. CCDC reference numbers 965089-965095. For ESI and crystallographic data in CIF or other electronic format see DOI: 10.1039/b000000x/

- 1 S. Lindskog, *Structure and Bonding*, Springer, Volume 8, 1970, pp 153-196; M. Kobayashi, S. Mhimizu, *Eur J Biochem.* 1999, **261**, 1.

- 2 F. B. Johansson, A. D. Bond, U. G. Nielsen, B. Moubaraki, K. S. Murray, K. J. Berry, J. A. Larrabee, and C. J. McKenzie, *Inorg. Chem.* 2008, **47**, 5079.
- 3 M. Murrie, *Chem. Soc. Rev.* 2010, **39**, 1986.
- 4 I. Krivokapic, M. Zerara, V. Daku, A. Vargas, C. Enachescu, C. Ambrus, P. Tregenna-Piggott, N. Amstutz, E. Krausz and A. Hauser, *Coord. Chem. Rev* 2007, **251**, 364; S. Hayami, Y. Komatsu, T. Shimizu, H. Kamihata and Y. H. Lee, *Coord. Chem. Rev.* 2011, **255**, 1981.
- 5 C. Boskovic, "Spin-Crossover Materials - Properties and Applications", M.A. Halcrow (Ed.), 2013, John Wiley & Sons, Chichester, UK, Chapter 7, 203-224; E. Evangelio, D. Ruiz-Molina, *Eur. J. Inorg. Chem.*, 2005, 2957.
- 6 J. J. M. Amoore, C. J. Kepert, J. D. Cashion, B. Moubaraki, S. M. Neville and K. S. Murray, *Chem. Eur. J.*, 2006, **12**, 8220; J. Olguin and S. Brooker, "Spin-Crossover Materials - Properties and Applications", M.A. Halcrow (Ed.), 2013, John Wiley & Sons, Chichester, UK, Chapter 3, 77-112.
- 7 S. Wagner, F. Kisslinger, S. Ballmann, F. Schramm, R. Chandrasekar, T. Bodenstein, O. Fuhr, D. Secker, K. Fink, M. Ruben and H. B. Weber, *Nature Nanotechnology*, 2013, doi:10.1038/nnano.2013.133; S. Fortier, J. J. Le Roy, C. -H Chen, V. Vieru, M. Murugesu, L. F. Chibotaru, D. J. Mindiola and K. G. Caulton *J. Am. Chem. Soc.*, 2013, **135**, 14670.
- 8 J. Tao, H. Maruyama and O. Sato, *J. Am. Chem. Soc.*, 2006, **128**, 1790.
- 9 S. Bin-Salamon, S. H. Brewer, E. C. Depperman, S. Franzen, J. W. Kampf, M. L. Kirk R. K. Kumar, S. Lappi, K. Peariso, K. E. Preuss and D. Shultz, *Inorg. Chem.*, 2006, **45**, 4461; N. G. R. Hearn, J. L. Korçok, M. M. Paquette and K. E. Preuss, *Inorg. Chem.*, 2006, **45**, 8817.
- 10 A. Bencini, C. A. Daul, A. Dei, F. Mariotti, H. Lee, D. A. Shultz and L Sorace, *Inorg. Chem.*, 2001, **40**, 1582.

11. A. L. Smith, K. I. Hardcastle and J. D. Soper, *J. Am. Chem. Soc.*, 2010, **132**, 14358; O. R. Luca and R. H. Crabtree, *Chem. Soc. Rev.*, 2013, **42**, 1440
12. K. G. Alley, G. Poneti, J. B. Aitken, R. K. Hocking, B. Moubaraki, K. S. Murray, B. F. Abrahams, H. H. Harris, L. Sorace and C. Boskovic, *Inorg. Chem.* 2012, **51**, 3944.
13. K. G. Alley, G. Poneti, P. S. D. Robinson, A. Nafady, B. Moubaraki, J. B. Aitken, S. C. Drew, C. Ritchie, B. F. Abrahams, R. K. Hocking, K. S. Murray, A. M. Bond, H. H. Harris, L. Sorace and C. Boskovic, *J. Am. Chem. Soc.*, 2013, **135**, 8304.
14. K. Chandrasenan and R. H. Thomson, *Tetrahedron*, 1971, **27**, 2529.
15. M. E. Bodini, P. E. Bravo and M. V. Arancibia, *Polyhedron*, 1994, **13**, 497.
16. C. Frontana, B. A. Frontana-Urbe and I. González, *J. Electroanal. Chem.*, 2004, **573**, 307.
17. C. Frontana and I. González, *J. Braz. Chem. Soc.*, 2005, **16**, 299.
18. P. Garge and S. Padhye, *Inorg. Chim. Acta*, 1989, **157**, 239.
19. S. Komboonchoo and T. Bechtold, *Color. Technol.*, 2011, **127**, 153.
20. G. Lamoureux, A. L. Perez, M. Araya, C. Agüero, *J. Phys. Org. Chem.*, 2008, **21**, 1022.
21. S. Salunke-Gawali, L. Kathawate, Y. Shinde, V. G. Puranik and T. Weyhermüller, *J. Mol. Struct.*, 2011, 1.
22. G. Valle-Bourrouet, V. M. Ugalde-Saldívar, M. Gómez, L. A. Ortiz-Frade, I. González and C. Frontana, *Electrochim. Acta*, 2010, **55**, 9042.
23. P. Garge, R. Chikate, S. Padhye, J. –M. Savariault, P. De Loth and J. –P. Tuchagues, *Inorg. Chem.*, 1990, **29**, 3315.
24. M. C. Rath, H. Pal and T. Mukherjee, *J. Chem. Soc., Faraday Trans.* 1996, **92**, 1891.
25. S. Salunke-Gawali, S. Y. Rane, V. G. Puranik, C. Guyard-Duhayon and F. Varret, *Polyhedron*, 2004, **23**, 2541.
26. S. Soares, S. S. Lemos, M. J. A. Sales, D. F. Back and E. S. Lang, *Polyhedron* 2009, **28**, 3811.

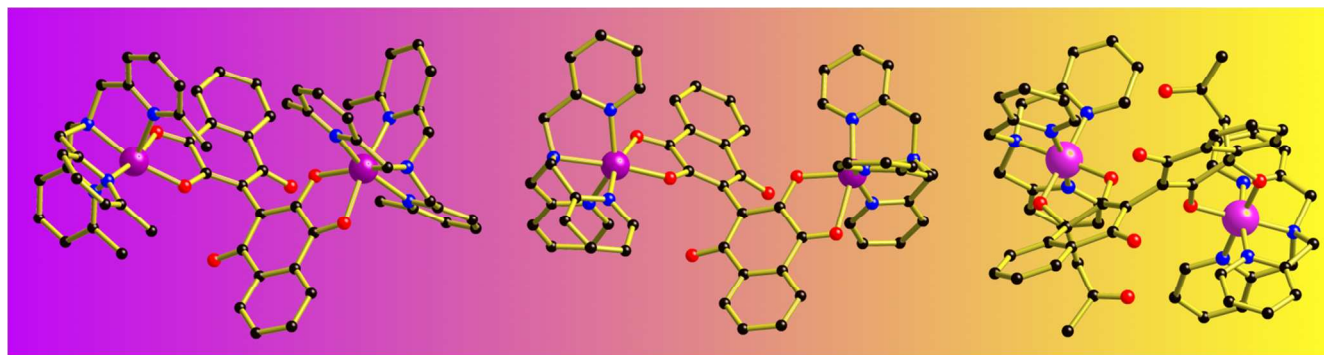
- 27 S. Y. Rane, S. Salunke-Gawali, A. S. Kumbhar, S. B. Padhyé and P. P. Bakare *J. Therm. Anal. Calorim.*, 1999, **55**, 249.
- 28 S. Salunke-Gawali, S. Y. Rane, K. Boukheddaden, E. Codjovi, J. Linarès, F. Varret and P. P. J. *J. Therm. Anal. Calorim.*, 2005, **79**, 669.
- 29 M. A. Ribeiro, M. Lanznaster, M. M. P. Silva, J. A. L. C. Resende, M. V. B. Pinheiro, K. Krambrock, H. O. Stumpf and C. B. Pinheiro, *Dalton Trans.*, 2013, **42**, 5462.
- 30 K. Yamada, S. Yagishita, H. Tanaka, K. Tohyama, K. Adachi, S. Kaizaki, H. Kumagai, K. Inoue, R. Kitaura, H. – C. Chang, S. Kitagawa and S. Kawata, *Chem. Eur. J.*, 2004, **10**, 2647.
- 31 K. Yamada, H. Tanaka, S. Yagishita, K. Adachi, T. Uemura, S. Kitagawa and S. Kawata, *Inorg. Chem.*, 2006, **45**, 4322.
- 32 L. Han, Y. Zhou and W. – N. Zhao, *Cryst. Growth Des.*, 2008, **8**, 2052.
- 33 R. Ishikawa, K. Yamada, S. Yamauchi, R. Miyamoto and S. Kawata, *Inorg. Chem. Commun.*, 2010, **13**, 636.
- 34 A. Blackman, *Eur. J. Inorg. Chem.*, 2008, 2633.
- 35 A. Beni, A. Dei, S. Laschi, M. Rizzitano and L. Sorace, *Chem. Eur. J.*, 2008, **14**, 1804.
- 36 D. T. Sawyer and J. L. Roberts, *Acc. Chem. Res.* 1988, **21**, 469.
- 37 J. L. Roberts, H. Sugimoto, W. C. Barrette and D. T. Sawyer, *J. Am. Chem. Soc.*, 1985, **107**, 4556.
- 38 G. S. Srivatsa and D. T. Sawyer, *Inorg. Chem.*, 1985, **24**, 1732.
- 39 J. A. Farrington, A. Ledwith and M. F. Stam, *Chem. Commun.*, 1969, 259.
- 40 S. Fukuzumi, I. Nakanishi, J. Maruta T. Yorisue, T. Suenobu, S. Itoh, R. Arakawa and K. M. Kadish, *J. Am. Chem. Soc.*, 1998, **120**, 6673.
- 41 M. C. Rath, H. Pal and T. Mukherjee, *J. Chem. Soc. Farad. Trans.*, 1996, 92, 1891.

- 42 C. Hormillosa, S. Healy, T. Stephen, and I. D. Brown, *Bond Valence Sum Calculator Version 2.00*, Institute for Materials Research, McMaster University, Ontario, Canada, 1993.
- 43 K. S. Murray, *Eur. J. Inorg. Chem.* 2008, 3101.
- 44 S. Salunke-Gawali, S. Y. Rane, K. Boukheddaden, E. Codjovi, J. Linares, F. Varret and P. P. Bakare, *J. Therm. Anal. Cal.*, 2005, **79**, 669.
- 45 S. E. Cheyne, L. F. McClintock and A. G. Blackman, *Inorg. Chem.* **2006**, *45*, 2610
- 46 C. –C. Zeng and J. Y. Becker, *J. Org. Chem.*, 2004, **69**, 1053.
- 47 H. –P. Schneider, W. Winter and A. Rieker, *J. Chem. Res.*, 1978, **336**, 3901.
- 48 M. A. Ernst-Russel, C. L. L. Chai, D. C. R. Hockless and J. A. Elix, *Aust. J. Chem.*, 1998, **51**, 1037.
- 49 E. Chosson, A. –E. Hay, A. Chiaroni, A. Favel, F. Tillequin, M. Litaudon and E. Seguin, *Heterocycles*, 2004, **63**, 2043.
- 50 G. –Y. Li, B. –G. Li, T. Yang, G. –Y. Liu and G. –L. Zhang, *Org. Lett.*, 2006, **8**, 3613.
- 51 J. Y. Cho, C. C. Kwon, P. G. Williams, P. R. Jensen and W. Fenical, *Org. Lett.*, **2006**, *8*, 2471.
- 52 O. Kahn, *Molecular Magnetism*, Wiley-VCH, Weinheim, Germany, 1993, 38; R. Boca, *Structure and Bonding*, 2006, **117**, 1.
- 53 W. A. Gobeze, V. A. Milway, N. F. Chilton, B. Moubaraki, K. S. Murray, S. Brooker, *Eur. J. Inorg. Chem.*, DOI:10.1002/ejic.201300368
- 54 M. Graf, G. Wolmershäuser, H. Kelm, S. Demeschko, F. Meyer and H. – J. Krüger, *Angew. Chem. Int. Ed.* 2010, *49*, 950.
- 55 R. L. Carlin, *Magnetochemistry*, Springer-Verlag New York, 1986, p 12.
- 56 R. M. Buchanan, C. G. Pierpont, *J. Am. Chem. Soc.*, 1980, **102**, 4951.
- 57 C. W. G. Ansell, J. Lewis, M. C. Liptrot, P. R. Raithby and M. Schroder, *J. Chem. Soc., Dalton Trans.* 1982, 1593.

- 58 H. Nagao, N. Komeda, M. Mukaida, M. Suzuki, K. Tanaka, *Inorg. Chem.*, 1996, **35**, 6809.
- 59 B. G. Gafford and R. A. Holwerda, *Inorg. Chem.*, 1989, **28**, 60.
- 60 C. Incarvito, M. Lam, B. Rhatigan, A. L. Rheingold, C. J. Qin, A. L. Gavrilova, B. Bosnich, *Dalton Trans.*, 2001, 3478.
- 61 Unit cell for partial single crystal X-ray structure determination for **7a**: Monoclinic, space group $P2_1/n$, $a = 13.7948(2)$ $b = 17.5128(3)$ $c = 29.1714(4)$ Å, $\beta = 101.359(2)$ °, $V = 6909.35(18)$ Å³, $Z = 4$, $T = 130(2)$ K.
- 62 G. M. Sheldrick, *SHELX97 Programs for Crystal Structure Analysis*; Institut für Anorganische Chemie der Universität, Tammanstrasse 4, D-3400 Göttingen, Germany, 1998.
- 63 *ABSPACK CrysAlis*, Oxford Diffraction Ltd., 2008.
- 64 A. L. Spek, Utrecht University: Utrecht, The Netherlands, 1998.

TOC Entry

Seven dinuclear cobalt complexes with bridging bis-bidentate naphthoquinone ligands reveal the steric influence of the ancillary capping ligand on the redox potential of the cobalt centres, with metal-catalysed derivatisation of the bridging ligand also observed.

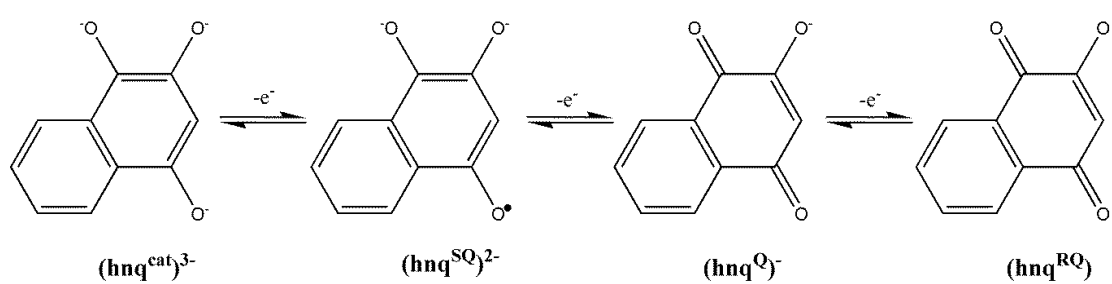


Supporting Information to accompany ...

Dinuclear cobalt(II) and cobalt(III) complexes of bis-bidentate naphthoquinone ligands†

**Yanyan Mulyana,^a Kerwyn G. Alley,^a Kristian M. Davies,^a Brendan F. Abrahams,^a
Boujemaa Moubaraki,^b Keith S. Murray^b and Colette Boskovic*^a**

Scheme S1. Different redox forms of the deprotonated hmqH ligand: diamagnetic catecholate ($\text{hnq}^{\text{cat}3-}$), radical semiquinonate ($\text{hnq}^{\text{SQ}2-}$), diamagnetic quinonate ($\text{hnq}^{\text{Q}-}$), and radical quinonate (hnq^{RQ}).



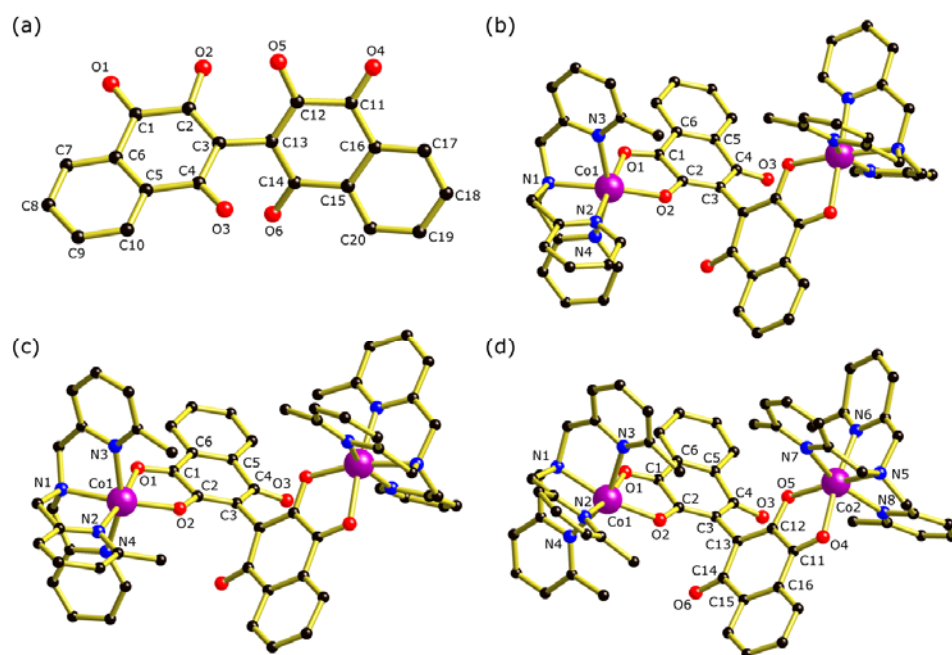


Figure S1. Structural representations of (a) bhnqH^+ in $(\text{pyH})(\text{bhnqH}) \cdot 2\text{H}_2\text{O}$ and complexes (b) **2** in $2\mathbf{a} \cdot 2\text{MeCN} \cdot 2\text{Et}_2\text{O}$, (c) **3** in $3\mathbf{a} \cdot 2\text{MeCN} \cdot \text{H}_2\text{O}$ and (d) **4** in $4\mathbf{a} \cdot 2\text{MeCN} \cdot 0.5\text{Et}_2\text{O}$.

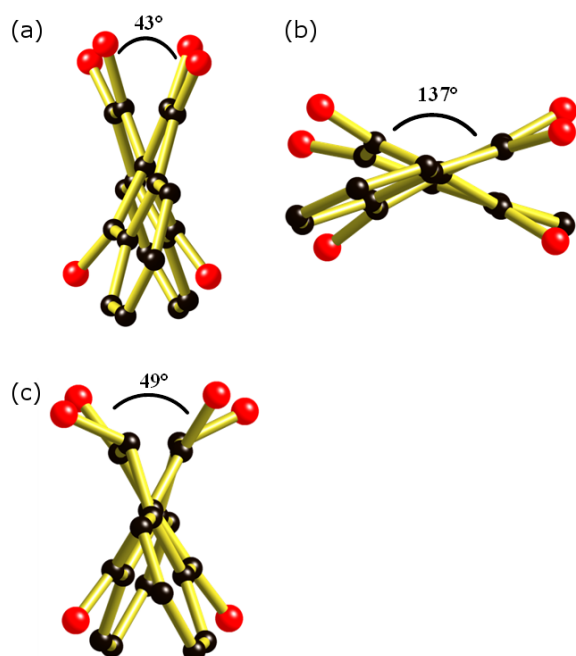


Figure S2. Dihedral angles of (a) bhnqH^+ in $(\text{pyH})(\text{bhnqH}) \cdot 2\text{H}_2\text{O}$, (b) bhnq^{2-} in $1\mathbf{b} \cdot 2\text{CH}_2\text{Cl}_2 \cdot 2\text{MeOH}$ and (c) bhnq^{2-} in $6\mathbf{a} \cdot 3\text{MeOH} \cdot 2\text{H}_2\text{O}$

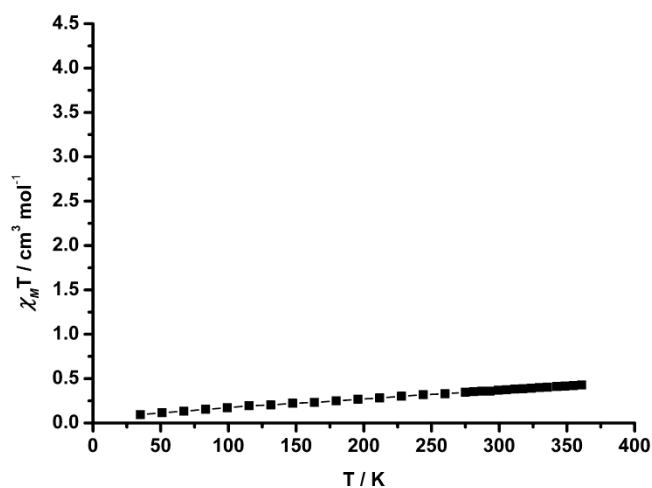


Figure S3. Magnetic susceptibility data measured for compounds **5b**·Me₂CO.

Table S1. Electronic absorption spectral data for acetonitrile solutions of bhnq²⁻ and compounds **1a**, **2a**, **3a**, **4a** and **5b** at ambient temperature.

Compound	$\lambda_{\max} / \text{nm} (\epsilon \times 10^3 \text{ M}^{-1} \text{ cm}^{-1})$
bhnq ²⁻	265 (27), 299 (sh, 1.8), 481 (4.9)
1a	258 (54), 303 (sh, 31), 348 (sh, 7.9), 498 (6.0)
2a	268 (44), 305 (sh, 21), 348 (sh, 6.3), 492 (5.1)
3a	271 (27), 307 (sh, 14), 350 (sh, 3.4), 520 (3.8)
4a	268 (28), 308 (sh, 14), 352 (sh, 4.6), 537 (4.2)
5b	246 (60), 280 (40), 325 (sh, 18), 378 (12), 614 (6.1)